International Journal of Nanomedicine

Dovepress
Taylor & Francis Group

Open Access Full Text Article

REVIEW

# Recent Advances in Near-Infrared Cyanine Dye-Based Fluorescent Nanoprobes for Tumor Imaging and Therapy

Yuxiang Gao[1], Lijun Zhu[1], Zhong Du[1], Jiabao Xiong[1], Rong Ma[2], Maierhaba Aili[2], Nuernisha Alifu[1,3], Biao Dong[3,4]

[1]The Second Affiliated Hospital of Xinjiang Medical University, The Second School of Clinical Medicine, Xinjiang Medical University, Urumqi, People's Republic of China; [2]The First Affiliated Hospital of Xinjiang Medical University, The First Clinical College of Xinjiang Medical University, Urumqi, People's Republic of China; [3]State Key Laboratory of Pathogenesis, Prevention and Treatment of High Incidence Diseases in Central Asia, School of Medical Engineering and Technology, Xinjiang Medical University, Urumqi, People's Republic of China; [4]State Key Laboratory on Integrated Optoelectronics, College of Electronic Science and Engineering, Jilin University, Changchun, People's Republic of China

Correspondence: Nuernisha Alifu; Biao Dong, Email nens_xjmu@126.com; dongb@jlu.edu.cn



**Abstract:** The early detection and high mortality rate of tumors have become great challenges in modern medicine. Recently, innovations in nanotechnology have provided a new paradigm in tumor accurate diagnosis and treatment. As the typical type of organic nanoprobes, near-infrared (NIR) cyanine dye-based fluorescent nanoprobes retain the inherent high luminescence efficiency and good biocompatibility of cyanine dyes. Due to their unique structure and excellent optical properties, some of them have been approved by the US Food and Drug Administration (FDA). Furthermore, cyanine dyes have exhibited dual photo-induced therapeutic functions of photothermal therapy (PTT) and photodynamic therapy (PDT). Notably, the high stability and tunable molecular structure of cyanine dyes allow for more stable binding to other contrast and therapeutic agents, expanding their use in biomedical diagnostics and therapeutics. To date, numerous studies have demonstrated the significant application potential of cyanine nanoprobes, garnering widespread attention from researchers. In this work, we provided a comprehensive overview of the novel applications of cyanine dye-based nanoprobes. Specifically, we discussed their unique properties and applications in fluorescence imaging, photoacoustic imaging, and multimodal tumor imaging. Additionally, we elucidate molecular design strategies, underlying mechanisms, and therapeutic applications of cyanine nanoprobes.

**Keywords:** cyanine dyes, near-infrared fluorescence, multimodal imaging, photothermal therapy, photodynamic therapy, combination therapy

## Introduction

Cancer remains one of the leading causes of death worldwide, posing a significant challenge to modern healthcare systems.[1] The inherent complexity, unpredictability, and heterogeneity of cancer lead to significant limitations to the effectiveness of diagnosis and treatment.[2–4] Although conventional imaging and conventional diagnostic methods have made some progress in early cancer detection, they still exhibit significant shortcomings.[5,6] Conventional therapeutic methods have shown ineffective results in cancer treatment, particularly in surgical resection. Surgical resection is one of the most commonly used approaches in cancer therapy.[7] However, this method faces numerous challenges in clinical practice, especially when tumor margins are unclear,[8,9] when micro-metastases are present,[10,11] or when tumors are inoperable due to their location or the patient's overall health condition.[12]

With the continuous advancement of materials science, nanotechnology has become an effective complement and innovative strategy for tumor detection and treatment properties, allowing for precise tumor targeting at the molecular level[13,14] and effective delivery of therapeutic molecules.[15] Meanwhile, NIR fluorescence imaging has emerged as a novel modality widely used in inflammation monitoring, vascular navigation, tumor imaging,[16] brain oxygenation

Received: 26 May 2025
Accepted: 15 October 2025
Published: 19 November 2025

and anesthesia depth assessment[17,18] This technique utilizes fluorescence probes with longer wavelengths, overcoming the limitations of conventional imaging methods. Organic fluorescence nanoprobes imaging primarily relies on emissions from the Near-Infrared I (NIR-I, 750–900 nm) and Near-Infrared II (NIR-II, 1000–1700 nm) regions.[19,20] These imaging methods provide clinicians and researchers with a non-invasive approach to observe and analyze deep tissues without causing harm to patients.[21,22] In particular, the NIR optical imaging has an excellent penetration ability in diagnosing and detecting highly invasive, widely metastasized and micro-metastasized tumor.[23] These progresses have given rise to a number of nanoprobe-based approaches to tumor diagnosis and treatment. To date, a series of organic and inorganic nanoprobes, including cyanine dyes,[24] single-walled carbon nanotubes (SWCNTs),[25] and quantum dots (QDs)[26] were adopted in the tumor field. Unfortunately, for many of these inorganic nanoprobes, there are inherent issues, like potential bio-toxicity risks, poor biocompatibility, and long-term retention inside patients' body.[27] Instead, organic nanoprobes do not have the problems listed above due to the inherently low toxicity[28] and good biocompatibility,[29] thus being biocompatible in vivo, with highly intensive in vivo fluorescence emission signals.[30] Therefore, the development of well-structured organic nanoprobes with strong NIR fluorescence performance, capable of meeting various tumor treatment needs, holds significant importance and potential in advancing integrated tumor diagnosis and therapy.

Among organic nanoprobes, cyanine dye-based nanoprobes have garnered increasing attention due to their efficient NIR fluorescence properties, excellent biocompatibility, and the ability to further optimize performance through substituent modifications.[31] A typical representative of these nanoprobes is indocyanine green (ICG),[32] the first NIR fluorescent dye approved by the US Food and Drug Administration (FDA), which has been widely applied in clinical diagnostics, particularly in tumor lymphatic imaging,[33] achieving significant results. Li et al[34] and Ren et al[35] developed targeted cyanine dye-based probes using IR820 and IR783, respectively, enabling high-sensitivity and long-duration in vivo imaging further validates the immense potential of cyanine dyes in tumor diagnostics. Cyanine dye-based nanoprobes not only show excellent optical properties, but also exhibit photothermal therapy (PTT) and photodynamic therapy (PDT) therapeutic properties.[36,37] Furthermore, the molecular structure of these nanoprobes is easily modifiable, allowing them to bind with targeting peptides,[38,39] antibodies, or drugs, further enhancing their accumulation in the target site and therapeutic effects. This integrated diagnostic and therapeutic functionality makes cyanine dye nanoprobes a comprehensive platform combining high-sensitivity imaging, precise targeting, and efficient treatment, providing strong technical support for integrated, precise tumor diagnosis and therapy.[40]

In recent years, fluorescence nanoparticles have been extensively investigated for their roles, applications, and imaging performance. For instance, Xu et al[41] and Zheng et al[42] reviewed recent advances in NIR fluorescent nanoprobes, highlighting their biomedical applications in tumor, vascular, and brain imaging, as well as their roles in image-guided therapy such as drug delivery, surgery, and phototherapy. However, these reviews primarily focus on NIR nanoprobes in general, with limited discussion on cyanine dye-based nanoprobes. In 2024,[43] An et al reviewed the progress of tumor combination therapy using cyanine nanoparticles from 2018 to 2023, discussing the design concepts, strategies, and challenges of cyanine dyes in order to promote clinical application research. However, this review primarily emphasized the therapeutic applications of the dyes and scarcely addressed their imaging and diagnostic applications.

Moreover, cyanine dye-based nanoprobes have garnered significant attention due to their strong NIR fluorescence, low toxicity, and excellent biocompatibility, making them highly promising for clinical applications such as imaging, therapy, and multimodal theranostics. Therefore, this review firstly summarized the physicochemical properties and limitations of cyanine dyes. Section 2 focuses on in vivo imaging, while Section 3 examines the roles in PTT/PDT and synergistic antitumor therapy when combined with other therapeutic agents. Finally, we discuss current challenges and future prospects for clinical translation. (Figure 1).

## Fundamentals of the Cyanine Dye

As the first-discovered dark blue fluorescent dyes with unique optical properties, cyanine dyes have rapidly become landmark achievements in the field of fluorescence imaging. Compared with quantum dots, rare earth-doped, and other fluorescent probes, cyanine dyes exhibited superior characteristics in terms of fluorescence performance and biocompatibility.[44] In this section, the history and optical properties of polymethylene dyes are

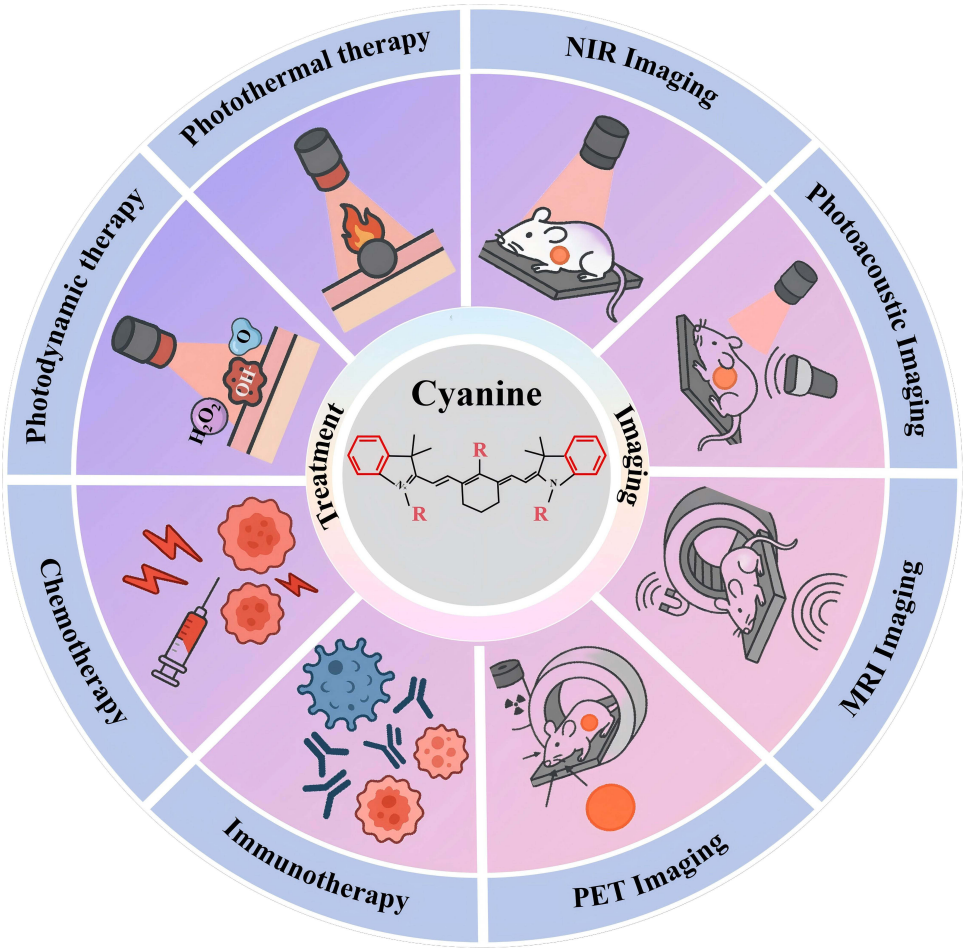


**Figure 1** Schematic illustration of the multifunctional applications of cyanine dye-based nanoprobes in tumor diagnosis and therapy. Right: Highlights the diverse imaging capabilities of cyanine nanoprobes, including NIR fluorescence imaging, PA imaging, and multimodal MRI/PET imaging. Left: Shows the therapeutic effects of cyanine nanoprobes via PTT/PDT and their synergy with other agents to enhance antitumor efficacy through combination therapies.

reviewed, and the assembly behaviour of polymethylene dyes at the molecular level is discussed in detail, especially the formation mechanism of H-aggregates and J-aggregates and their modulation of photophysical properties. On this basis, this section will further discuss other molecular design strategies and nanoconstructive approaches that have been used to enhance the performance of polymethylene dyes in recent years, including the introduction of conjugated extended structures, and self-assembling mediators, in order to realise their highly efficient applications in biomedical fields (Figure 2).

## Development Process and Characteristics of Cyanine Dyes

Cyanine dyes are renowned for their unique molecular structures.[45] Generally, these fluorophores consist of two nitrogen-containing heterocyclic groups at their ends, which are connected by a conjugated poly-methyl chain.[46] These dyes are known for their distinctive optical properties, including narrow absorption and emission bands (λmax/λem),[47] high molar extinction coefficients,[48] and minimal Stokes shifts.[49]

In 1856,[50,51] Charles-Hansen-Grivell-Williams synthesized the first cyanine-9 dye. By distilling quinine from cinchona bark, he obtained quinoline and reacted it with pentyl iodide and excess ammonia, resulting in a vivid blue compound, later named quinoline blue. With the continued exploration of cyanine fluorescent dyes, researchers gradually synthesized various cyanine dyes with differing structures. The earliest cyanine dyes were types with methylamine and dimethylamine, containing one or two methylamine units in the conjugated chain between heterocycles, absorbing visible light in the range of 450–520 nm.[52] Later, researchers developed cyanine dyes like CY3, CY5, and CY7 (Figure 3A),


https://doi.org/10.2147/IJN.S542880

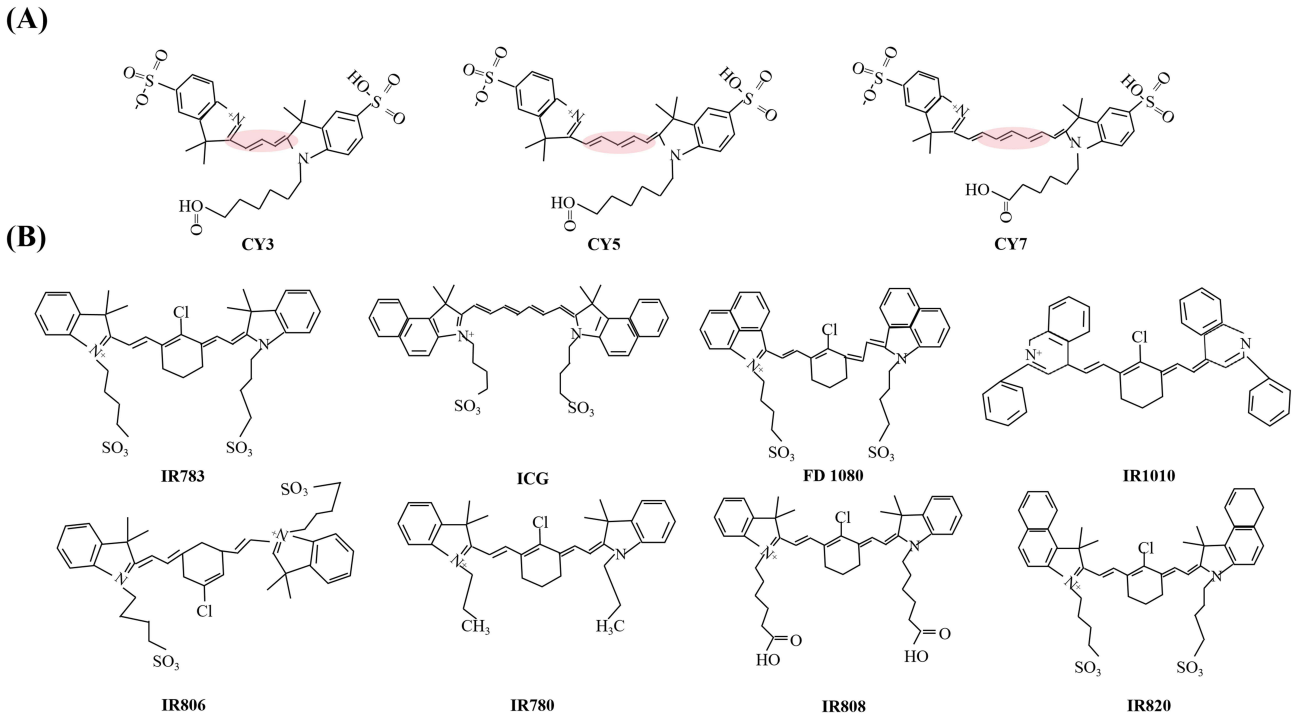


**Figure 2** (**A**) Chemical structure of CY3, CY5 and CY7. (**B**) Different kinds of cyanine dyes.

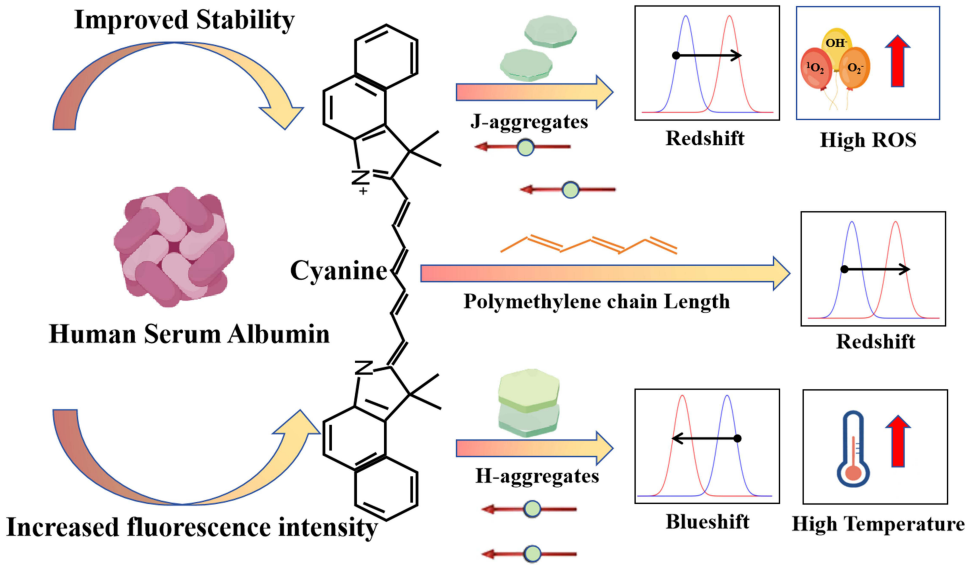


**Figure 3** The effects of J aggregates (red shift of absorption peak and improvement of PDT) and H aggregates (absorption peak blue shift and enhanced PTT) on cyanine dyes, and other methods (conjugated extended structures and protein-based self-assembly) for regulating their properties.

which were named based on the length of their conjugated poly-methyl chains.[53–55] In addition to classification based on the length of the conjugated poly-methyl chain, researchers further classified these dyes based on other characteristics. They can be categorized into symmetric or asymmetric polymethine dyes depending on the substituents at both ends.[24] Furthermore, based on whether the methyl chain contains rigid ring structures (such as cyclopentane, cyclopentene, or cyclohexene), polymethine dyes can be either linear or non-linear. With the deepening understanding of the structure and properties of cyanine fluorescent dyes, their application range has expanded. Indocyanine green (ICG),[56] due to its excellent safety and biocompatibility, was one of the first used for in vivo NIR imaging and is the first fluorescent dye

approved by the FDA for clinical human use. The clinical value of ICG has been thoroughly validated in numerous human studies, providing an important foundation for the subsequent applications of cyanine dyes. Building upon this, researchers have continued to employ a variety of high-performance polymethine dyes for in vivo NIR imaging applications, including IR783, ICG, FD1080, IR1010, IR806, IR780, IR808 and IR820 (Figure 3B).[57,58] Moreover, these dyes not only exhibit significant absorption and emission peaks in the NIR-I, but researchers have also discovered that these dyes can show high fluorescence intensity in the NIR-II, with extended emission tailing.[59,60] This unique NIR-II characteristic enables deeper tissue penetration and higher imaging resolution, providing more powerful tools for biomedical imaging and diagnostics.

## J-Aggregates and H-Aggregates

In recent years, more and more properties of cyanines have been discovered. One of the most important findings is that elanine is able to form supramolecular structures of H-aggregates or J-aggregates by self-incorporation at different concentrations in different solutions. According to Kasha's exciton theory,[61] generally speaking, the slip angle of J-aggregates is less than 54.7° and that of H-aggregates is more than 54.7°. In terms of spatial structure and spectral characteristics, H-aggregates are arranged in parallel between the molecules, and the absorption peaks show blue shifts, while J-aggregates are arranged in a head-to-tail arrangement between the molecules, and the absorption peaks show red shifts. The formation of these aggregates can be precisely controlled by modulating the concentration of the solution, the temperature and the nature of the solvent, which allows precise control of the manner in which the cyanine aggregates, thus achieving specific optical properties in different environments.

In 2019,[62] Sun et al have found that 1,2-dimyristoyl-sn-glycero-3 phosphocholine (DMPC) can effectively help FD1080 to form J-aggregates, and the optimal molar ratio was found to be 1:20. In 2024,[63] Mohammed R prepared J-aggregates using 8 mg/mL (10.3 mm) of ICG in solution, which was heated at 65°C for 24 hours before being concentrated to 50 mg/mL of J-aggregates that had formed ICG. The realisation of this aggregate resulted in a significant redshift of the absorption wavelength of ICG, avoiding the overlap with the absorption of haemoglobin. Moreover, the application of aggregates in addition to improve the spectral properties and stability of cyanine dyes, Peng's group[64] discovered an cyanine dye-based photosensitiser (IDMQ), which can automatically form J aggregates in negatively charged microenvironments, and they found that J aggregates are not only important for red-shifting the dye but also for enhancing PDT. However, H aggregates do not always have a negative impact. Although H aggregates can lead to fluorescence quenching, they have an important modulating role in improving the PTT or PDT properties of materials. The molecules of H aggregates are usually arranged in a face-to-face stacking arrangement with strong overlapping π-orbitals, an arrangement that allows H aggregates to accelerate heat generation through a non-radiative energy decay mechanism, resulting in excellent photothermal conversion efficiencies. For example, Wu et al[65] introduced fluorescein and tetraphenylethylene (TPE) groups and guided the formation of H-type aggregates of the Cy7 molecule via rapid injection. Compared to the monomeric form of Cy7, these supramolecular assemblies exhibited significantly enhanced photothermal conversion. The photothermal conversion efficiencies (PCE) of Cy7–TPE and Cy7–pyrene were reported to be 9.5% and 22.3%, respectively. This finding further underscores the great potential of H-aggregates in the field of photothermal energy conversion.

## Modification and Performance Enhancement of Cyanine Dyes

Structural modifications to the aromatic rings, the central polymethylene chain, or the incorporation of functional groups such as hydroxyl, amino, or carboxyl groups, as well as biological macromolecules, such as proteins, peptides, carbohydrates, can endow cyanine dyes with diverse functionalities and physicochemical properties. Modulation of the absorption and emission wavelengths of cyanine dyes is one of the important means to increase the potential of fluorescent dyes for clinical applications. The main objective is to increase the redshift (shift of the absorption spectrum to longer wavelengths) by increasing the conjugation system in the cyanine dye molecule to reduce the energy difference between the highest occupied molecular orbital (HOMO) and the lowest unoccupied molecular orbital (LUMO) in the molecule. Lei's research[66] team investigated and designed CX, an organic fluorescent dye based on cyanine dyes, and in further studies found that for every two carbon atoms added to the conjugated linkage, the absorption and emission

wavelengths were red-shifted by about 100 nm, and that the absorption/emission wavelengths of CX-3 (polymethylene chain length of 3) both exceeded 1000 nm. However, the extension ability of the polymethyl chain in cyanine dyes is not unlimited. Studies have shown that when the number of consecutive methyl groups in the methyl chain exceeds 7, the "cyanine limit" effect is triggered, that is the molecule will break symmetry after exceeding a critical length.[67,68] In addition, the researchers also found that human serum albumin (HSA)[69,70] enhances the fluorescence properties of cyanine dyes. In 2022,[31] Tian et al discovered that the cyanine dye IR-783 binds even more effectively to a specific part of HSA. Experimental results showed that the fluorescence enhancement in the HSA DIII region combined with the cyanine dye IR-783 was 1.6 times higher than that of the mixture of HSA and IR-783. Moreover, other research teams have also reported that HSA can enhance its fluorescence intensity in combination with cyanine dyes. Moreover, other research teams have also reported that HSA can be combined with cyanine dyes to enhance their fluorescence intensity. For example, Li's team and Zhu's team reported that the fluorescence intensity of IR820@HSA and IR780@HSA was increased by 21-fold and 24-fold, respectively, compared to their own fluorescence intensities.[71,72] This finding further underscores the significant role of HSA in modulating the fluorescence properties of cyanine dyes, offering new insights into the development of efficient fluorescent probes and biomarkers. For PTT and PDT, Sheng et al[73] demonstrated that HSA can stably bind with the cyanine dye ICG to form intelligent nanocomplexes, which significantly enhance both PTT efficiency and reactive oxygen species (ROS) generation for PDT. This synergistic enhancement improves the synergistic therapeutic effect of ICG, thereby achieving more efficient tumour ablation.

## Cyanine Dye Based Nanoprobes for Tumor Imaging Applications

Cyanine dye based nanoprobes have emerged as powerful tools in the field of in vivo tumor imaging due to their unique optical properties, such as strong NIR absorption, high fluorescence quantum yield, and excellent biocompatibility.[74] These nanoprobes leverage the deep tissue penetration and minimal background autofluorescence provided by the NIR window to achieve high-resolution imaging of tumor lesions with enhanced contrast. Furthermore, by integrating cyanine dyes into nanocarriers, these nanoprobes have paved the way for multimodal imaging techniques,[75] combining NIR fluorescence with other imaging modalities such as and photoacoustic imaging (PAI), positron emission tomography (PET), and magnetic resonance imaging (MRI). Therefore, this section offers a comprehensive review of the use of nanoprobes based on cyanine based fluorescent dyes for fluorescence imaging and multimodal tumor imaging (Table 1).

### NIR Fluorescence Imaging of Tumors with Cyanine Nanoprobes

Cyanine dyes, particularly those in the NIR window, are widely used due to their significant advantages in molecular imaging. These dyes, when combined with other molecules to form novel nanoprobes, significantly enhance the imaging performance for solid tumour detection, sentinel lymph node localisation, early detection of distant metastases, and imaging of haematological tumours. Specifically, probes such as ICG@BSA and 5H5 enhance NIR fluorescence imaging of solid tumours; probes like LJ-GSH and PMT9 can precisely identify metastatic cancer lesions and lymph nodes; and probes such as Cy5 and IR-26 target specific mutations and leukaemia cells, supporting real-time monitoring and precision therapy. In summary, cyanine dye-based nanoprobes demonstrate significant potential in various tumour diagnostics. Although these probes show great promise, further optimising their performance in deep tissue imaging and clinical applications remains a key focus for future research.

#### Solid Tumour Imaging Based on NIR Cyanine Nanprobes

NIR fluorescence imaging has significant advantages such as low background noise, strong tissue penetration and high sensitivity. It is especially suitable for diagnosing and monitoring the dynamic changes of tumors, and provides powerful technical support for early diagnosis. Cervical cancer, as the second most common gynecological malignancy affecting women worldwide, urgently requires the development of a fluorescent nanoprobe for early diagnosis.[94] In 2021,[76] R. Ma et al developed albumin-based nanoprobes (ICG@BSA) composed of bovine serum albumin (BSA) and ICG. Compared to free ICG at the same concentration, ICG@BSA exhibited enhanced NIR fluorescence intensity (Figure 4A). In vivo experiments in mice also demonstrated strong NIR fluorescence emission from cervical tumors and the liver, whereas no fluorescence signal was detected in the PBS-treated control group. Therefore, the excellent NIR fluorescence imaging

**Table 1** Application of Cyanine Based Nanoprobes in Tumour Imaging

| Imaging Method | Nanoprobes | Absorption/ Emission Peak (nm) | Imaging Application | Maximum TNR, SBR, SNR | RT/ Clearance Pathways | Advantage | Ref. |
|---|---|---|---|---|---|---|---|
| NIR | BSA@ICG-DOX | 745/840 | Cervical tumour | – | 48h/Liver | Deep penetration | [76] |
| NIR | YQ-04-03 | 780/810 | Breast and liver tumour | 3.95 (TNR) | 48h/Liver | High contrast | [77] |
| NIR | 5H5 | 1069/1125 | Glioma and tumour vessels | 7.2 (SBR) | 24h/ Hepatobiliary | In situ diagnosis | [78] |
| NIR | ICG@Lips-cRGD | 805/850 | Glioma | – | – | Precision diagnosis | [79] |
| NIR | LJ-GSH | 782/815 | Lung metastasis of breast cancer | 7.2 (SBR) | 48h/Live | Precision guidance | [80] |
| NIR | PMT9 | 650/780 | Lung/Glioma/ Pancreatic cancer | – | 24h/- | Metastasis diagnosis | [81] |
| NIR | β-LG@IR-780/ BSA@IR-780 | –/910 | Lymph nodes and lymphatic vessels | | 24h/Renal/ Hepatobiliary | Highlight lymph | [82] |
| NIR | LPP-QDs-IR-820 | 819/1350 | Lymphatic system | 4.16 (SNR) | 72h/Liver and kidney | Lymphoscintigraphy | [58] |
| NIR | Vem-L-Cy5 3 w | 640/655-665 | Leukemia | – | – | Cell detection | [83] |
| NIR | IR-26 | 775/805 | Acute myeloid leukemia | – | – | Target imaging | [84] |
| NIR | D/INPs@CM | –/- | Multiple myeloma | – | 48h/Liver | Marrow tracking | [85] |
| PAI | FP700 | 797/836 | Cervical cancer | – | 6h/ Hepatobiliary | Dual-modal imaging | [86] |
| PAI | CY7.5 | –/- | Breast cancer/ Cholangiocarcinoma | – | – | pH-responsive | [87] |
| PAI | IR806-RGD | 808/855 | Breast cancer | 58.4 (NIR) | 24h// Hepatobiliary | Brain imaging | [88] |
| PAI | IR-32P | 1094/1120 | Glioma | 11 (NIR) | 24h/Hepatic and renal | Targeting-enhanced | [89] |
| NIR+MRI | NPs-Ate | 780/800 | Breast cancer | 11.51(NIR)/1.95 (MRI) | 72h/Liver and kidney | Response imaging | [90] |
| NIR+MRI | Fe3O4@mSiO2-ICG/cMBP | –/- | Breast cancer | 13.6(NIR) | 48h/- | Metastasis imaging | [91] |
| NIR+MRI | IUFP | 1012/1039 | Breast cancer | – | 36h/Liver | Multimodal imaging | [92] |
| NIR+PET | IR808-DOTA | 776/800 | Breast cancer | 8 (PET) | 72h/Renal | PET/NIR imaging | [93] |

**Abbreviations**: TNR, Tumor-to-normal tissue ratio; SBR, Signal background ratio; SNR, Signal-to-Noise Ratio; NIR, Near-Infrared; PAI, Photoacoustic Imaging; MRI, Magnetic Resonance Imaging Imaging; PET, Positron Emission Tomography RT, Residence time of nanoprobes in the body; CP, Nanoprobes Metabolic Pathwa.

capabilities of ICG@BSA provide significant support for early detection and targeted diagnosis of cervical cancer, potentially reducing misdiagnosis and missed diagnosis (Figure 4B). In 2024,[77] Lin et al used a new cyanine fluorescent probe, YQ-04-03, to perform NIR imaging of tumours in mouse models of breast and liver cancer. The experimental results showed that the 24-hour imprinted light intensity TNR of YQ-04-03 in the breast cancer model was significantly higher than that of the ICG group, and YQ-04-03 also demonstrated good fluorescence properties in the liver cancer model. In addition to breast cancer and liver cancer, human gliomas are also one of the major challenges currently facing the early diagnosis of tumors. Due to their special location and unclear boundaries, gliomas are often difficult to accurately identify with high resolution and specificity in imaging tests. In 2019, Ding et al developed a novel fluorescent probe, 5H5 (Figure 4C),[78] which exhibited excellent imaging performance in a human glioblastoma mouse model, enabling clear visualization of both the tumor tissue and intratumoral microvasculature (Figure 4D). Subsequently, Guo et al[79] demonstrated that an innovative nanocomposite platform, ICG@Lips-cRGD, provides high-resolution imaging in

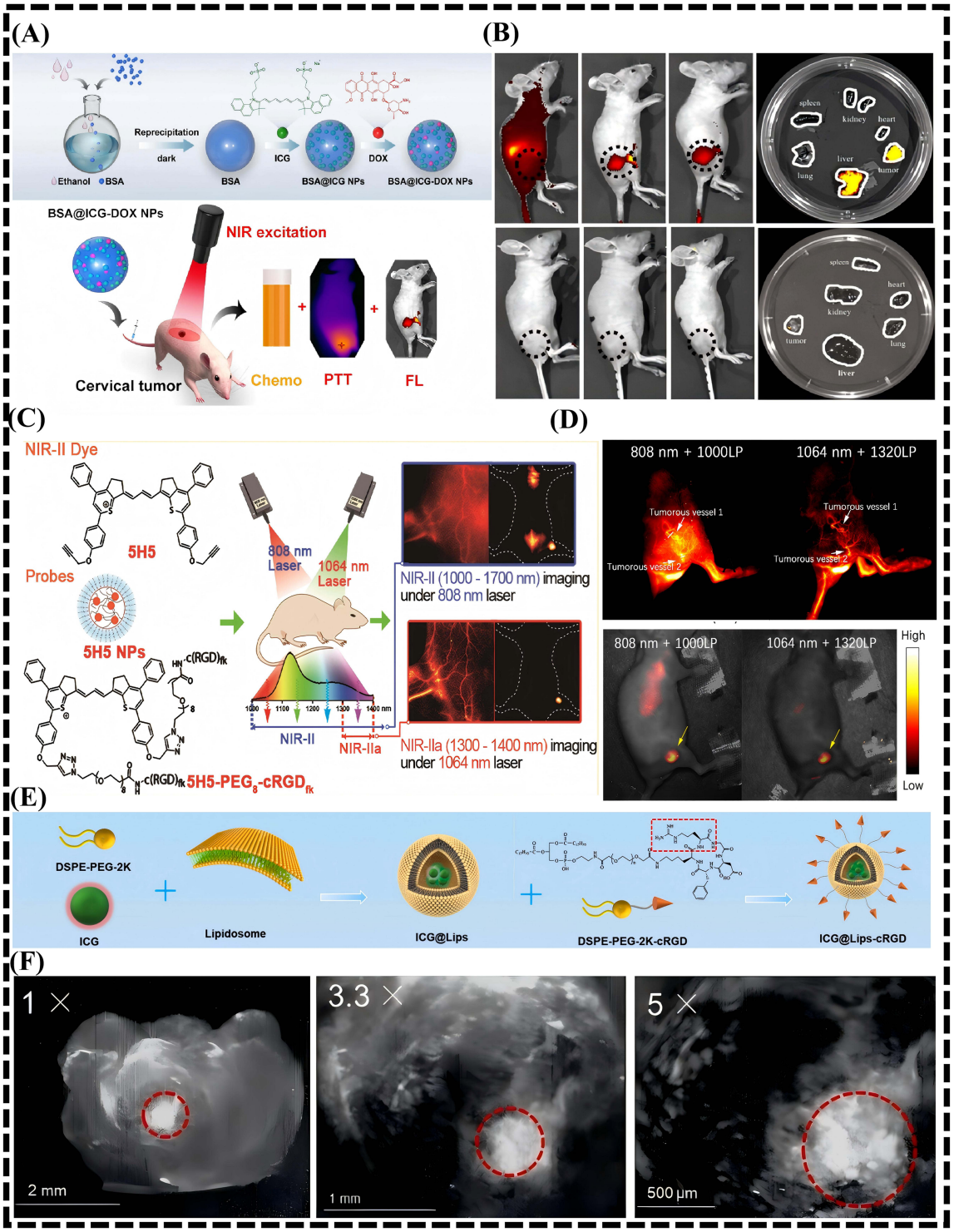


**Figure 4** (**A**) Schematic illustration of the synthesis of BSA@ICG-DOX nanoparticles and their application in tumor thermal imaging and fluorescence imaging. (**B**) NIR fluorescence images of tumoured nude mice and major organs injected with BSA@ICG NPs (black dotted circles are subcutaneous tumor site). Reproduced from Ma R, Alifu N, Du Z et al. Indocyanine Green-Based Theranostic Nanoplatform for NIR Fluorescence Image-Guided Chemo/Photothermal Therapy of Cervical Cancer. Int J Nanomedicine. 2021 Jul 17;16:4847–4861. Copyright 2021, Ma. Creative Commons Attribution – Non Commercial.[76] (**C**) Schematic illustration of the synthesis of 5H5 nanoparticles and their application in NIR imaging. (**D**) Tumour imaging with 5H5 NPs under 808 nm laser irradiation (yellow arrows indicate tumour vessels and the tumour site). Reproduced from Ding B, Xiao Y, Zhou H et al. Polymethine thiopyrylium fluorophores with absorption beyond 1000 nm for biological imaging in the second near-infrared subwindow. J Med Chem, 2018, 62:2049–2059. Copyright © 2018 American Chemical Society.[78] (**E**) Schematic synthesis of ICG@Lips-cRGD. (**F**) NIR-II fluorescence images of brain tumour tissue sections (red dotted circle indicates the tumour). Reproduced from Guo L, Zhou Y, Ding J, Wang Y, Li J, Wang Y et al. A near-infrared triggered multi-functional indocyanine green nanocomposite with NO gas release function inducing improved photothermal therapy. J Colloid Interface Sci, 2025, 679:307–323. © 2022 by the authors. Licensee MDPI, Basel, Switzerland. This article is an open access article distributed under the terms and conditions of the Creative Commons Attribution (CC BY) license (https://creativecommons.org/licenses/by/4.0/).[79]

both ectopic and in situ tumour models (Figure 4E). For ectopic tumours, the NIR fluorescence signal at the tumour site was significantly stronger, enabling precise localisation and enhanced imaging contrast. In the in situ tumour model, the in situ glioma was sectioned and processed nearly, and the results showed that the NIR-II fluorescence signal at the tumour site could be observed at 1x objective, 3.3x objective and 5x objective (Figure 4F). The cyanine dye based fluorescence probes, with their high contrast and resolution in NIR fluorescence imaging, hold promise for more accurate tumor detection and localization. However, these probes still face challenges in deep tissue imaging.

## Tumour Metastasis and Sentinel Lymph Node Monitoring Based on NIR Cyanine Nanprobes

The use of NIR fluorescence imaging technology for the monitoring of tumour metastasis and the localization of sentinel lymph nodes has become a key research area in tumour diagnosis and treatment. Cyanine based nanoprobes can accurately detect small metastases and sentinel lymph nodes, help to detect small metastases at an early stage, optimize treatment strategies, reduce unnecessary extensive lymph node dissection, lower the risk of distant metastasis, and improve treatment outcomes. Metastasis is the main cause of death in cancer patients, and early identification of small metastatic lesions can significantly improve patient survival. For this problem, Wang et al[80] designed a nanoprobes, LJ-GSH (Figure 5A), based on the cyanine dye Cy7, to detect the location of lung metastases in breast cancer. In in vivo mouse experiments, the glutathione (GSH) levels in the lung metastases were significantly elevated, allowing LJ-GSH to effectively target the metastatic sites. NIR imaging revealed a high signal-to-background ratio (SBR), demonstrating that LJ-GSH has the potential to differentiate metastases from adjacent lung tissue. In another study, jia et al[81] developed an IR780-based lung metastasis nanoprobe (PMT9) (Figure 5B). In this study, the breast tumour site could be clearly distinguished from the adjacent normal lung tissue at 2 hours after PMT9 injection, and remained quite bright after 24 hours, with almost negligible background signal. The authors also used PMT9 to detect lung metastases from glioma and lung metastases from pancreatic cancer. In the lung metastasis model of glioma and in the lung metastasis model of pancreatic cancer, PMT9 similarly accurately illuminated the metastases rather than normal tissue, with a significant SBR. In addition, PMT9 not only demonstrated excellent capabilities in the detection of single metastases in the lung, but also in the visualisation of multiple metastases in the lung tissues, confirming the efficacy of PMT9 for the imaging of lung metastases (Figure 5C). Next, the application of these two probes expanded the potential of cyanide nanoprobe technology in the ultra-sensitive monitoring of the lymphatic system. In 2023, Xu et al[82] employed two probes, β-lactoglobulin@IR-780 (β-LG@IR-780) and bovine serum albumin@IR-780 (BSA@IR-780), for lymphatic NIR-II imaging, successfully visualizing lymph nodes and lymphatic vessels. Both probes exhibited extended imaging windows and demonstrated excellent NIR-II lymphatic imaging capabilities even at low power densities. Compared with simple imaging of solid tumours,[95] accurate imaging of the lymphatic system surrounding cervical cancer tumours is more important in clinical diagnosis and treatment. In the study by Zhu,[58] a LPP-QDs-IR-820 nanoprobes (Figure 5D) based on cyanine based fluorescent dyes was developed and successfully applied for high-resolution real-time imaging of the lymphatic system and cervical tumors in the NIR region. These nanoprobes exhibited exceptional NIR fluorescence quantum yield and excellent fluorescence stability. In vivo experiments, the probe not only clearly delineated the contours of cervical tumors but also achieved high-resolution imaging of the lymphatic system (Figure 5E). Notably, the nanoprobes enabled real-time monitoring of the lymphatic drainage process under high signal-to-noise ratio conditions, providing a powerful tool for the diagnosis and treatment of cervical cancer. Cyanine dye based nanoprobes have demonstrated excellent performance in efficient imaging and precise identification of sentinel lymph nodes and metastasis, significantly enhancing their value in early tumor diagnosis and surgical navigation. However, the mechanisms behind their ability to recognize sentinel lymph nodes and metastasis have not been thoroughly investigated, and a consensus has yet to be reached.

## NIR Imaging of Haematological Malignancies Based on Cyanine Nanprobes

In haematological malignancies, conventional diagnostic methods may be highly effective in detecting solid tumours, and often may face shortcomings of insufficient sensitivity and specificity for haematological malignancies. Therefore, NIR imaging based on cyanine nanoprobes offers new opportunities for early detection and monitoring of haematological malignancies. The team of Poliseno and Taliani[83] synthesized and validated a cyanine dye based nanoprobes, Vem-

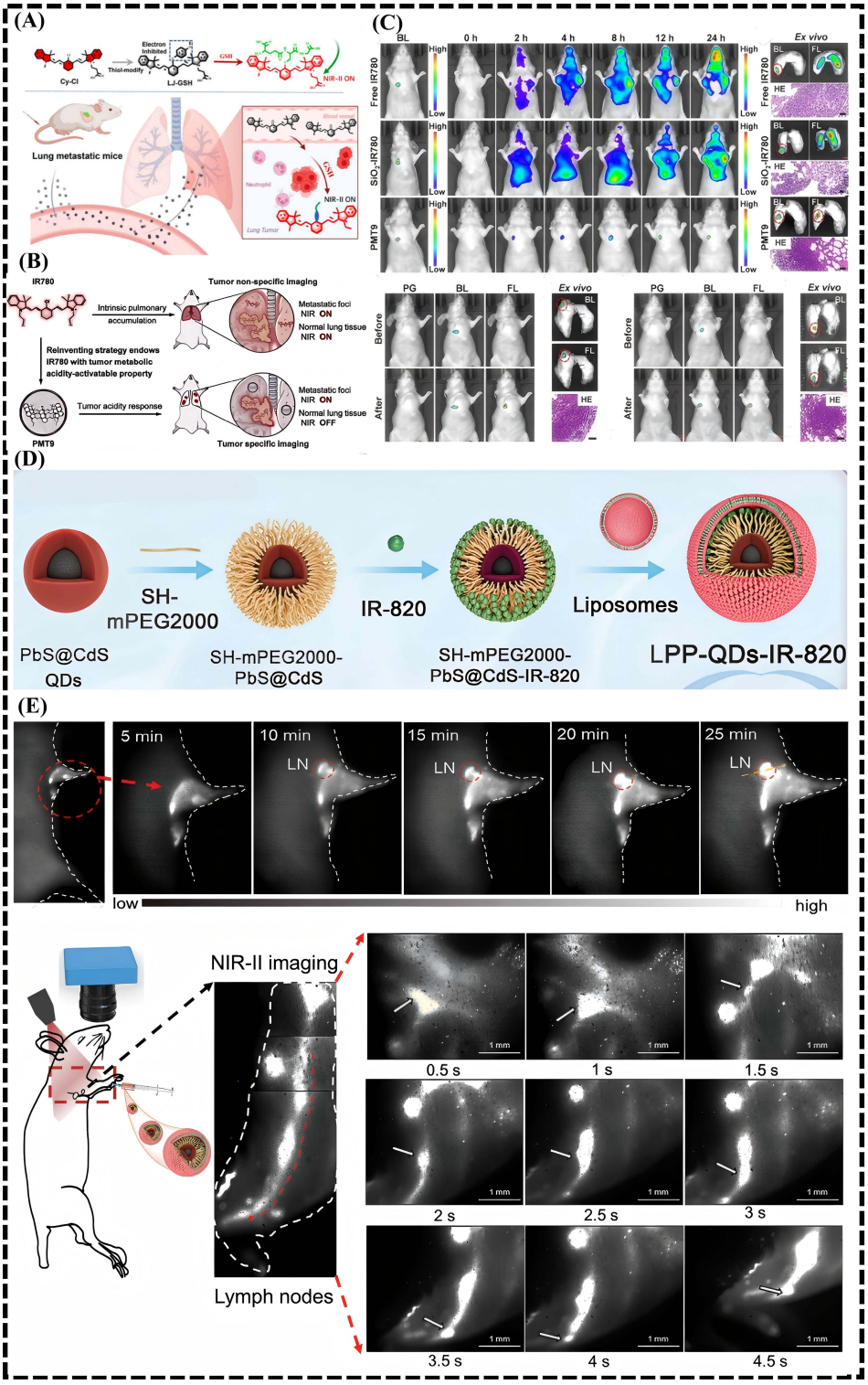


**Figure 5** (**A**) Schematic representation of the probe LJ-GSH design and response strategy and of the mechanisms involved in the diagnosis of lung metastatic lesions. Reproduced from Wang Y, Zhao G, Liu Y et al. Glutathione-activated near-infrared II fluorescent probe for lung metastatic diagnosis and intraoperative imaging of tumor. Sens Actuators B Chem, 2025, 426:137005. Copyright 2025, Wang.[80] (**B**) Schematic representation of the PMT9 probe for NIR imaging of lung-associated tumours. (**C**) Evaluation of PMT9 for imaging lung metastases in vivo *(red circles indicate tumour tissue)*. Reproduced from Jia Q, Zhang R, Yan H et al. An activatable near-infrared fluorescent probe for precise detection of the pulmonary metastatic tumors: A conventional molecule having a stunning turn. Angew Chem, 2023, 135:e202313420. © 2023 Wiley-VCH GmbH.[81] (**D**) Illustration of LPP-QDs-IR-820 NCs synthesis process. (**E**) NIR-II fluorescence images of LPP-QDs-IR-820 NCs enriched with lymphocytes and chronological recording of the lymphatic drainage process (red circles indicate lymphoid tissue) (white dotted line indicates the lymphatic margin). Reproduced from Zhu L, Du Z, Xiong J, Li H, Zhang C, Zhang X et al. Phototheranostic LPP-QDs-IR-820 nanocomposites for specific NIR-II imaging of lymphatic and photothermal therapy of cervical tumors. Adv Healthc Mater, 2024, 13:2401358. *© 2024 Wiley-VCH GmbH.*[58]

L-Cy5, for the detection of BRAFV600E mutations in cancer cells. The BRAFV600E mutation, which is found in various cancers, including hairy cell leukemia, was specifically targeted by this nanoprobes. This nanoprobes penetrates cancer cells and selectively binds to BRAFV600E, exhibiting a binding affinity comparable to that of the conventional therapeutic agent vemurafenib, while addressing some of the limitations associated with vemurafenib. As a fatal haematological malignancy, acute myeloid leukaemia is a disease with rapidly progressive symptoms and a high degree of recurrence. Zhang et al[84] synthesized a series of derivatives based on heptamethine cyanine dyes, among which IR-26 exhibited a remarkably high mitochondrial targeting ability in acute myeloid leukemia (AML) cells. Confocal microscopy observations revealed that IR-26 preferentially accumulated in AML cells, a characteristic observed across various AML cell lines, while no such phenomenon was detected in normal peripheral blood mononuclear cells (PBMCs). In vivo, the probe successfully localized HL-60 (lentivirus-transfected) tumor xenografts in mice. Furthermore, by establishing a human AML mouse model, the NIR in vivo flow cytometry (IVFC) system was employed for detection, using GFP fluorescence as an internal reference. IR-26 efficiently detected NIR fluorescent leukemia cells in vivo. The successful application of this probe provides a novel method for real-time monitoring of the progression of AML. In 2024, Gao et al[85] designed a cyanine-based nanoprobes (D/INPs@CM) for the treatment of another hematologic malignancy (multiple myeloma) (Figure 6A). In both in vitro and in vivo experiments, D/INPs@CM, which is coated with the cell membrane of multiple myeloma (MM) cells, was shown to easily penetrate the bone marrow cavity and subsequently target tumor cells. With good cellular compatibility, D/INPs@CM showed no hemolysis. In vivo, DiRNPs@CM nanoparticles exhibited significantly high fluorescence intensity in the multiple myeloma (MM) orthotopic transplantation model and mouse femur tissue, fully confirming their ability to effectively localize and accumulate in MM tumor tissues (Figure 6B and C). Although these nanoprobes may exhibit limited selectivity for specific subtypes or molecular markers, they have demonstrated excellent targeted imaging capability in blood malignancies such as acute myeloid leukemia and multiple myeloma, providing crucial support for the precise diagnosis and real-time monitoring of hematologic cancers.

## Photoacoustic Imaging of Cyanine Dyes in Living Organisms

NIR PAI is a new non-destructive biomedical imaging technology that combines the advantages of optical imaging and acoustic imaging, and has higher spatial resolution and contrast than other imaging techniques. In addition to imaging laser-activated fluorescent materials using only NIR, ultrasonic signals can also be generated after the laser-activated materials are excited. This two-modal imaging technology that combines optical and acoustic techniques not only gives PAI the high sensitivity of fluorescence imaging, but also the deep penetration and high resolution of ultrasound imaging.[89] Compared with conventional optical imaging methods, PAI can break through the limitations of optical scattering and provide clearer structural information on deep tissues.[96] Notable advances include the FP700 probe, which offers higher 3D imaging resolution and better tissue penetration than conventional fluorescence imaging. Another pH-responsive cyanine dye (cysteine) is used for tumour-specific PAI, achieving high sensitivity and high contrast. The IR806-RGD probe enhances breast cancer diagnosis through dual-modality imaging, demonstrating prolonged tumour retention time. The IR32p probe successfully penetrates the skull to achieve deep glioma imaging, showing better contrast and tissue penetration.

In 2023,[86] Zou et al designed and synthesized a probe FP700 that combines a cyanocyanine dye and a 2,4-dinitrobenzenesulfonyl group. The FP700 probe is capable of PAI to penetrate deeper tissue layers and provide high-resolution three-dimensional imaging as compared to conventional fluorescence imaging. In addition, PAI reduces the effect of light scattering and provides clearer information about tumor boundaries. Combined with fluorescence imaging, FP700 has great potential for real-time dynamic monitoring and deep lesion diagnosis (Figure 7A). In 2024,[87] unlike the FP700 probe which then triggers photoacoustic and fluorescent signals in response to recognition of cysteine (Cys), the Tsuchiya team designed and synthesized a set of pH-responsive cyanocarbocyanine dyes for PAI of cancer cells. When these dyes encountered the acidic environment of tumor cells, the absorption spectra and photoacoustic signals changed significantly, providing accurate pH-dependent PAI. The article's research shows that these probes were successfully applied to PAI of cancer cells and were able to effectively differentiate between healthy and tumor tissues, especially by responding to the acidic environment to achieve high sensitivity and high contrast imaging. In 2023,[88] The

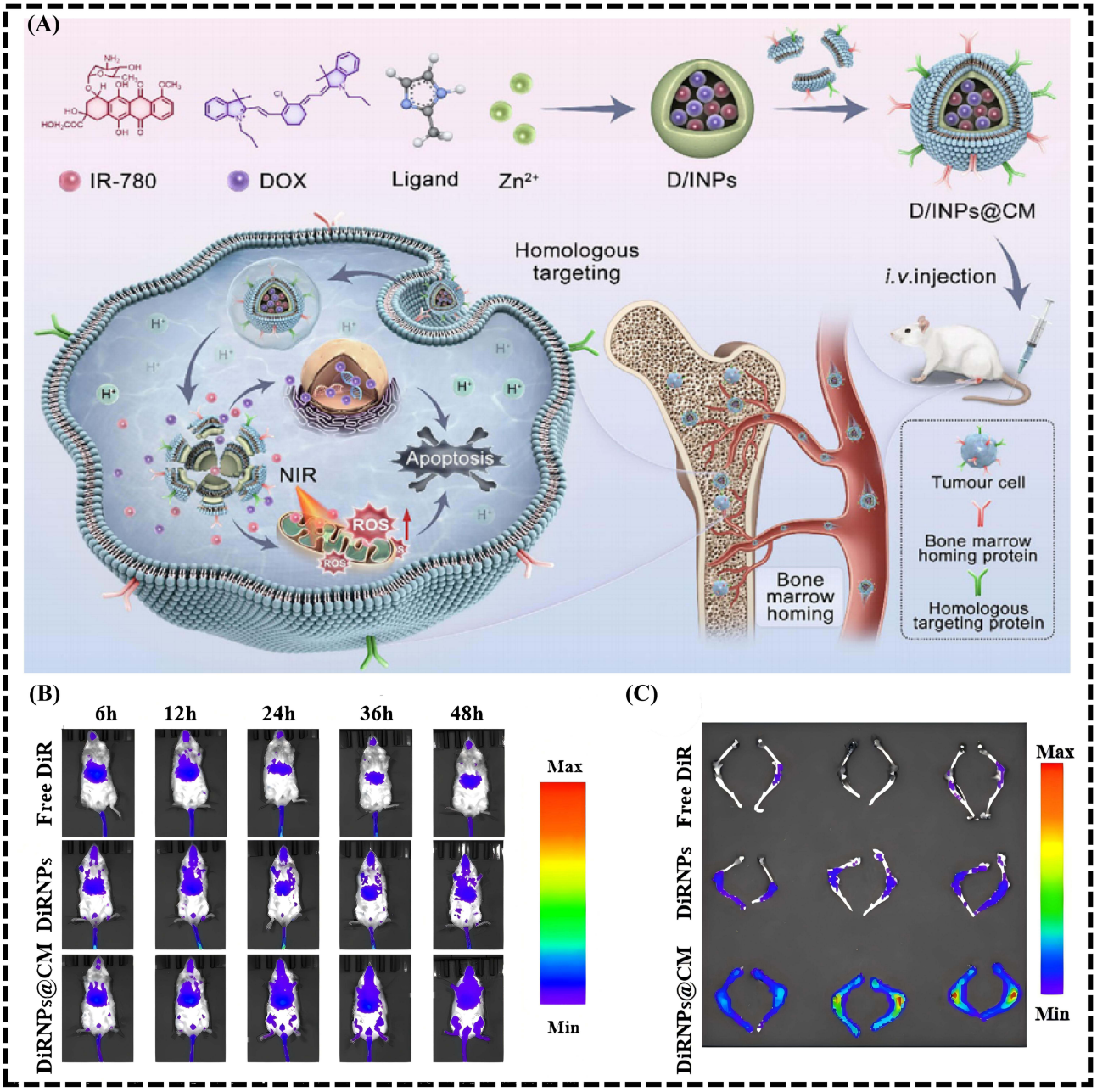


**Figure 6** (**A**) Preparation of D/INPs@CM and its application in multiple myeloma targeting (red upward arrow indicates an increase in reactive oxygen). (**B**) Fluorescence imaging was used to assess the in vivo distribution of nanoparticles in an orthotopic multiple myeloma model. (**C**) In vitro the femoral tissue of injected H929-luc mice. Reproduced from Gao G, Che J, Xu P, Chen B, Zhao Y. Biomimetic cell membrane decorated ZIF-8 nanocarriers with IR-780 and doxorubicin loading for multiple myeloma treatment. Aggregate, 2024, 5:e631. © *2024 The Author(s). Aggregate published by SCUT, AIEI, and John Wiley & Sons Australia, Ltd. Creative Commons CC BY license.*[85]

researchers designed and synthesized a probe called IR806-RGD. By introducing the RGD group to the anthracene dye IR806, its ability to target tumours was enhanced (Figure 7B). Studies have shown that IR806-RGD exhibits a longer emission wavelength, higher fluorescence intensity and excellent breast cancer tumour targeting under the NIR-II. In vivo imaging experiments have shown that this probe not only provides high-contrast images of breast cancer tumours in NIR-II fluorescence imaging, but can also be used for PAI, thereby achieving more comprehensive imaging of breast cancer tumours. The data on PAI showed that in the 4T1 tumour mouse model, after intravenous injection of IR806-RGD, the photoacoustic signal in the tumour area gradually increased, reaching a maximum 12 hours after injection, with an enhancement of 1.78 times, which significantly improved the imaging contrast compared to the baseline signal before

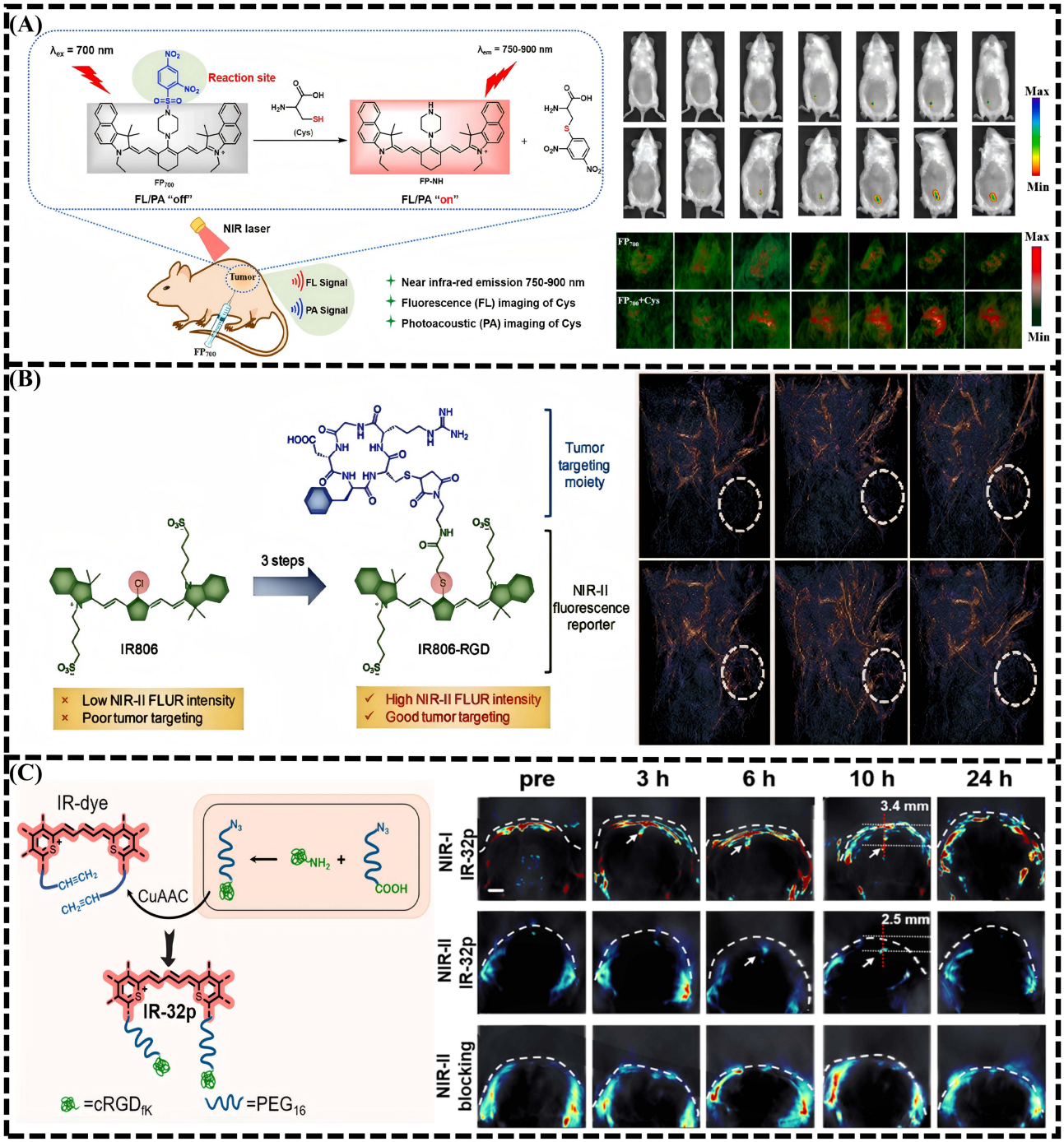


**Figure 7** (**A**) Schematic diagram of the synthesis of probe FP700, and *in vivo* FL images and PA imaging in mice. Reproduced from Zou X, Zhao Y, Lin W. Photoacoustic/fluorescence dual-modality cyanine-based probe for real-time imaging of endogenous cysteine and in situ diagnosis of cervical cancer in vivo. Anal Chim Acta, 2023, 1239:340713. © *2022 Elsevier B.V. All rights reserved.*[86] (**B**) Schematic structure and synthesis of IR806-RGD and In vivo PA imaging (white circle indicates tumour tissue). Reproduced from Liu Y, Lu X, Zhou W et al. Molecular engineering of a commercially available NIR-II fluorescent cyanine dye for improved tumor targeting and imaging. New J Chem, 2023, 47:20088–20094. Copyright 2023, Royal Society of Chemistry (RSC); ROYAL SOCIETY OF CHEMISTRY.[88] (**C**) Schematic representation of the synthesis of IR-32p and the NIR-I/II PA imaging after IR-32p injection. Reproduced from Lyu S, Lu S, Gui C et al. A NIR-II photoacoustic/NIR-IIa fluorescent probe for targeted imaging of glioma under NIR-II excitation. J Med Chem, 2024, 67:1861–1871. Lyu S, Lu S, Gui C, Guo C, Han J, Xiao Y et al. A NIR-II photoacoustic/NIR-IIa fluorescent probe for targeted imaging of glioma under NIR-II excitation. J Med Chem, 2024, 67:1861–1871. Copyright © 2024 American Chemical Society.[89]

injection. Even after 24 hours, the photoacoustic signal remained at a high level, demonstrating the good targeting and long-lasting tumour retention of the probe. However, imaging the brain is particularly challenging compared to other tissues due to the presence of the skull and complex brain structures, which hinder light penetration and signal clarity. In 2024,[89] Lyu et al developed an αvβ3 integrin-targeted NIR-II photoacoustic/NIR-IIa fluorescent probe, IR32p

(Figure 7C), based on a cyanine dye, for the targeted imaging of gliomas. In experiments conducted on mouse models, IR32p was found to effectively penetrate the skull, enabling deep glioma imaging. Notably, under 1020 nm laser excitation, the probe demonstrated superior imaging contrast and deeper tissue penetration compared to NIR-I imaging. IR32p was able to achieve tissue penetration of approximately 2.5 mm in NIR-II PAI, with an 8-fold higher tumor-to-normal tissue signal ratio compared to NIR-I imaging, underscoring its potential for targeted glioma imaging. From the perspective of this nanoprobes, which combines photoacoustic imaging and NIR imaging, the combination of the two imaging modes helps to obtain more comprehensive and accurate diagnostic information about tumors, significantly improving the accuracy of imaging and its potential for clinical application.

## Multimodal Imaging of Cyanine Dyes in Living Organisms Using Fluorescence/MRI/PET

NIR imaging-based tumor diagnosis has been widely studied due to its numerous advantages. However, it still faces certain limitations in detecting tumor anatomical structures, functional status, and molecular characteristics. By combining NIR imaging with other established modalities such as MRI and PET, these limitations in resolution, specificity, and multidimensional information acquisition can be effectively addressed.[97] For example, NPs-Ate, IUFP, and Fe3O4@mSiO2-ICG/cMBP nanoprobes combine NIR fluorescence with MRI imaging to achieve precise multimodal imaging of tumors and lymphatic tissues. In contrast, the IR808-DOTA probe integrates NIR fluorescence with PET for successful tumor localization and surgical guidance. The combined use of these nanoprobes significantly enhances tumor imaging and real-time monitoring capabilities.

In 2023,[90] Liu et al developed a dual-modality imaging technology based on a nanoprobe, termed NPs-Ate (Figure 8A), which combines the PD-L1-targeting monoclonal antibody Atezolizumab, the NIR dye ICG, and the MRI contrast agent Gd-DTPA for the precise imaging of triple-negative breast cancer (TNBC). The nanoprobe demonstrated significant progress in NIR-II and MRI dual-modality imaging by achieving precise tumor localization through the high-sensitivity fluorescence detection in the NIR-II region and high-resolution MRI. In tumor-bearing mice, NIR-II imaging reached a peak SBR of 11.51 at 36 hours post-injection, indicating high imaging contrast. In the MRI modality, the nanoprobe exhibited a maximum SBR of 1.95 at 12 hours (Figure 8B–D). In tumor imaging research, in addition to precise localization and imaging of the tumor itself, the detection of lymph node metastases is equally critical. Lymph nodes are one of the primary pathways for tumor dissemination, making their accurate imaging of significant clinical importance for the early diagnosis and assessment of tumor metastasis. In 2024,[91] Wang et al also developed a c-Met-targeted dual-mode nanoprobe for NIR-II fluorescence and MRI imaging to accurately diagnose and monitor metastasis in TNBC. The probe Fe3O4@mSiO2-ICG/cMBP integrates a superparamagnetic Fe3O4 nanocore with a mesoporous silica shell, which is loaded with the clinically approved NIR-II dye ICG and modified with a c-Met-targeting binding peptide (cMBP). Studies have shown that this probe can effectively target TNBC metastases. The entire lymphatic process of in vivo TNBC metastasis has been accurately imaged, and excellent NIR-II fluorescence signals have been achieved, with an optimal signal-to-background ratio (SBR) of 13.6. The T1-weighted MRI contrast is significantly higher than that of conventional agents such as Gd-DTPA. In terms of imaging stability, compared with the conventional MRI contrast agent Gd-DTPA, the Fe3O4@mSiO2-ICG/cMBP probe can maintain a high signal intensity for 6 hours after administration, and the relative signal intensity of the target group rapidly increases to three times that of Gd-DTPA after 2 hours. In 2024,[92] researchers developed a new multifunctional nanoprobe called IUFP NPs, which is based on a newly designed cyanine dye IR-1010 and integrates upconversion nanoprobes (UCNPs) and perfluorooctanoic acid-15-crown-5 ether (PFCE), which can be used for both NIR-II fluorescence imaging and nuclear magnetic resonance imaging. The innovative design of IR1010 combines an electron donor group, which achieves a high quantum yield (3.08%) and excellent photostability. IUFP nanoprobes simultaneously exhibit both NIR-II fluorescence and upconversion luminescence under single-wavelength excitation, thereby improving the imaging of small tissues such as blood vessels and lymph nodes. In addition, this nanoprobe also has effective PAI and MRI capabilities. Experiments have shown that the in vitro MRI intensity is linearly correlated with the concentration of IUFP NPs, confirming that this probe can achieve accurate tumor imaging and in vivo monitoring. In addition to MRI, cyanine dye-based nanoprobes can also be combined with a variety of functional materials to successfully achieve multimodal applications of PET and fluorescence imaging. In 2023,[93] Zhu et al developed a dual-modal imaging probe (Figure 8E), IR808-DOTA, combining the NIR-II heptamethine dye IR808 with the chelating agent DOTA. This probe, labeled with Gallium-68, allowed

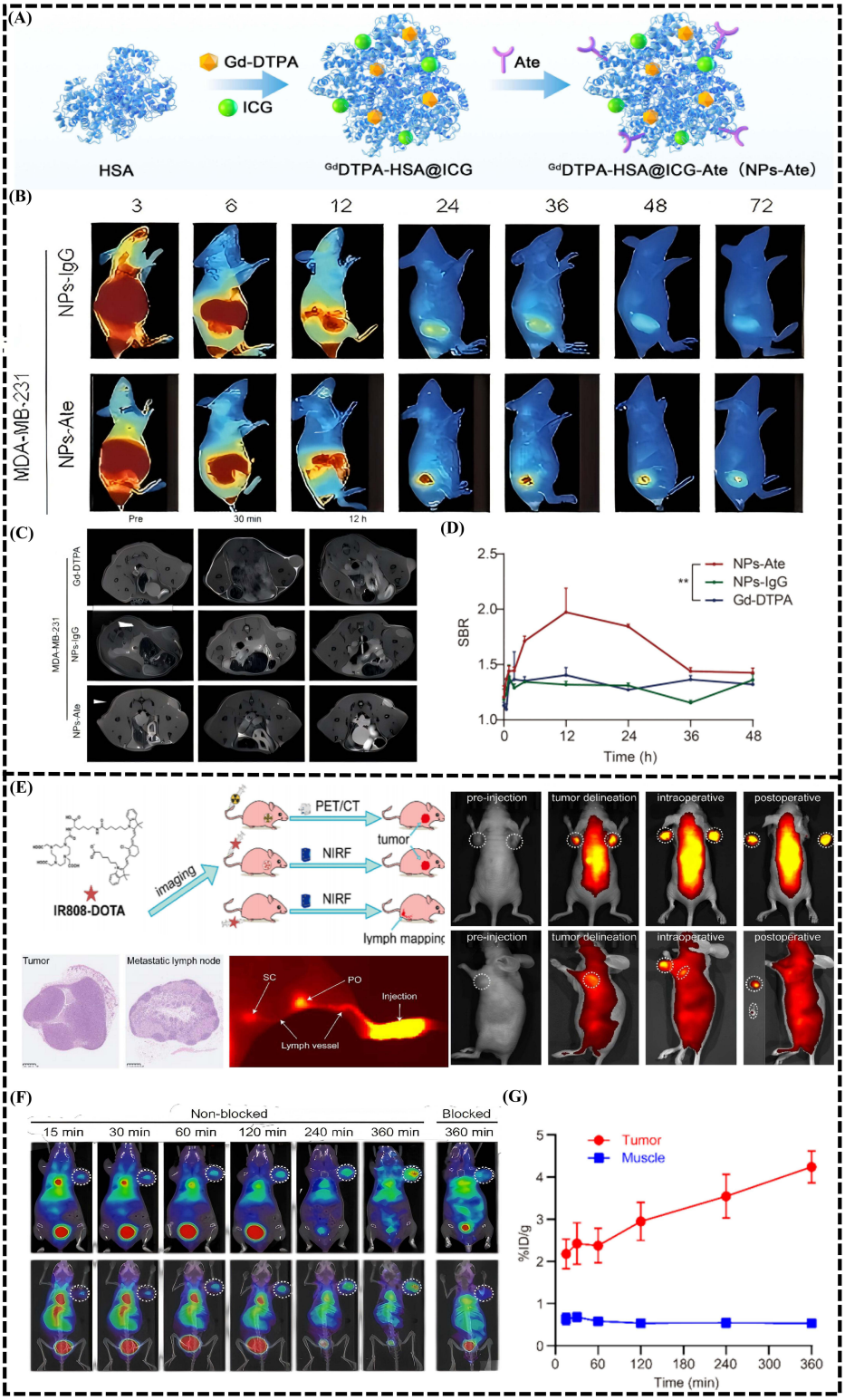


**Figure 8** (**A**) NPs-Ate research workflow. (**B**) In vivo NPs-Ate fluorescent imaging. (**C**) In vivo NPs-Ate MRI imaging and (**D**) signal-to-noise ratio (SBR) images of MDA-MB-231 tumour-bearing mice at various times. Reproduced from Liu WL, Zhang YQ, Luo XJ et al. Novel dual-mode NIR-II/MRI nanoprobe targeting PD-L1 accurately evaluates the efficacy of immunotherapy for triple-negative breast cancer. Int J Nanomedicine, 2023, 18:5141–5157. Copyright 2023, Liu et al. Creative Commons Attribution – Non Commercial.[90] (**E**) Precise resection of tumours and metastatic lymph nodes under NIR imaging with IR808-DOTA, validated by H&E staining and lymph node mapping. (**F**) PET/CT images of MCF-7 tumour-bearing mice after injection of IR808-DOTA and corresponding quantitative analyses (**G**). Reproduced from Zhu J, Liu Y, Li W, Xu C, Zhang T, Zhao H. In vivo evaluation of a gallium-68-labeled tumor-tracking cyanine dye for positron emission tomography/near-infrared fluorescence carcinoma imaging, image-guided surgery, and photothermal therapy. ACS Omega, 2023, 8:6067–6077. Copyright © 2023 The Authors. Published by American Chemical Society. This publication is licensed under CC-BY-NC-ND 4.0.[93]


https://doi.org/10.2147/IJN.S542880

simultaneous PET and NIR fluorescence imaging. The study demonstrated that IR808-DOTA achieved precise tumor localization in MCF-7 tumor-bearing mice, offering a high contrast with a tumor-to-muscle ratio greater than 8 at 360 minutes post-injection. The probe provided deep tissue PET imaging and high-resolution NIR imaging for intraoperative guidance (Figure 8F and G), effectively delineating tumor margins and visualizing sentinel lymph nodes. These results highlight the probe's potential in guiding tumor resection and monitoring therapy in real time. The combination of NIR fluorescence imaging with MRI and PET significantly enhances the accuracy of tumor and metastasis localization and diagnosis. However, how to extract useful information from the integrated data remains a crucial challenge for improving diagnostic precision and clinical decision-making.

## Cyanine Dye-Based Nanomedicines in Tumor Therapy Applications

Nanomedicines based on cyanine dyes not only utilize the NIR absorption and fluorescence properties of these dyes to achieve deep tissue penetration, high-resolution imaging, and precise PTT and PDT therapies, but they also enable the integration of cyanine dyes into nanocarriers.[98] This integration enhances the stability and bioavailability of the dyes while allowing the incorporation of additional therapeutic agents, such as chemotherapeutic drugs, immunomodulators, or gene therapy vectors.[99] This multifunctional approach demonstrates significant advantages in achieving synergistic effects for tumor therapy. This section presents the PTT and PDT mechanisms of nanoprobes based on cyanine based fluorescent dyes, along with a detailed discussion on the application and efficacy of these fluorescent probes in PTT therapy, PTT/PDT combination therapy, and their potential implications for chemotherapy and immunotherapy.

### Mechanisms of PTT and PDT Based on Cyanine Dyes

For PTT, cyanine dyes can function as conventional photothermal agents primarily due to their unique optical and molecular structural characteristics.[100] Firstly, cyanine dyes have a highly conjugated π-electron system,[101] giving them a high extinction coefficient.[102,103] This strong absorption property enables efficient photon capture under NIR irradiation, facilitating deep tissue photothermal conversion.[104] Secondly, upon absorbing photons, electrons in cyanine dyes are excited to a higher energy state. Rather than returning to the ground state through radiative transitions, these excited electrons release energy as heat, thereby raising the local temperature.[105] In contrast for PDT, cyanine dyes primarily induce ROS via a Type I reaction mechanism, relying on electron transfer by photosensitizers. Upon absorbing light energy, the dyes transition from the ground state to an excited triplet state.[106–108] In this state, photosensitizers can transfer electrons to surrounding molecules or oxygen, generating superoxide anions ($O_2^-$)[109] and hydroxyl radicals (-OH).[110] A key feature of the Type I mechanism is its lower dependence on oxygen levels, making it effective even in hypoxic tumor microenvironments.[111] On the other hand, in the Type II mechanism of PDT, cyanine dyes primarily rely on energy transfer to molecular oxygen.[112,113] Upon photon absorption, photosensitizers transfer energy directly to form singlet oxygen ($^1O_2$).[114] However, this reaction requires a higher concentration of oxygen, potentially limiting its efficiency in hypoxic conditions within tumors.[115,116] The combination of these two mechanisms enables cyanine dyes to generate ROS under varying oxygen conditions, thereby enhancing the overall efficacy of PDT (Figure 9).

### PTT Treatment with Cyanine Nanprobes

In PTT, treatment is divided into high-temperature therapy and low-temperature mild therapy. For high-temperature therapy, the primary mechanism involves raising the local temperature of the tumor to 42 °C or higher, which can lead to the destruction of cancer cells by inducing heat-mediated protein denaturation.[117] For example, in 2023,[118] Yang and others developed a multifunctional nanoplatform (MGCN) called "Golden Cicada" and made significant progress in photothermal tumor therapy (Figure 10A). The team of researchers designed and synthesized an ICG-based polyethyleneimine (PEI)-modified HSP70 gene silencing system. MGCN downregulates HSP70 expression, disrupts the thermal impedance mechanism of tumor cells, and achieves efficient targeted enrichment of ICG. Under NIR laser (808 nm) irradiation, MGCN exhibits excellent photothermal conversion performance. In the mouse B16-F10 melanoma model, the temperature at the tumor site can be increased to about 47°C after injection, thereby significantly inhibiting tumor growth (Figure 10C). Through this photothermal gene therapy strategy of cascaded enhanced synergistic effect', MGCN

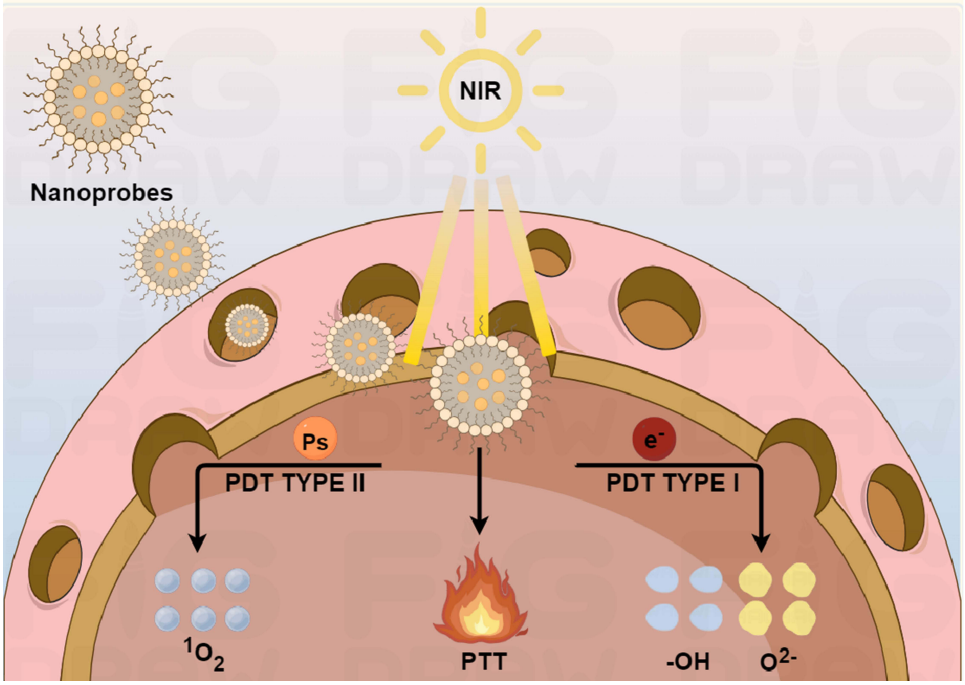


**Figure 9** Schematic illustration of heat generation and ROS production by cyanine dyes under NIR laser irradiation.

exhibits excellent anti-tumor activity both in vitro and in vivo, effectively overcoming the thermal resistance of tumors. For hyperthermia treatment, higher temperatures can more effectively kill tumour cells.[119,120] In 2023,[121] Wang et al developed a biomimetic photothermal agent based on heptamethylcyanine dye, named Lipo-PTO (Figure 10B), for targeted treatment of breast cancer by PTT. This bionic photothermal agent is designed to specifically respond to low pH and high ROS levels in the tumour microenvironment. Under these conditions, the liposomal shell is broken down, releasing Cy-NTf, which is converted to Cy-NH, thereby activating its photothermal properties. Studies have shown that this system has a photothermal conversion efficiency of up to 42.09% under 650 nm laser irradiation, and the temperature rises significantly to 64°C. In vivo experiment on 4T1 breast cancer mice, Lipo-PTO combined with laser irradiation completely ablated the tumours in the tumour treatment group, with no recurrence for 22 days (Figure 10D), while the tumours in the control group continued to grow, with minimal impact on surrounding healthy tissue. For cyanine dyes, the form of the aggregate may affect its photothermal properties. In 2024,[122] Feng and his team designed a photothermal agent based on platinum coordination self-assembly with cyanine dye. They synthesized two dimers: CyMe-Pt and CyEt-Pt, of which CyMe-Pt formed tightly packed J-aggregates by replacing ethyl groups with methyl groups to reduce steric hindrance. This design resulted in significant structural changes, which improved the photothermal conversion efficiency. It was found that under 980 nm laser irradiation, the temperature of CyMe-Pt could rise to about 60 °C, which could significantly inhibit tumor growth. Compared with CyEt-Pt, CyMe-Pt has a more prominent photothermal therapeutic effect. In vivo experiments, the growth of mouse tumours in the CyMe-Pt treatment group was effectively suppressed, and the tumour volume was significantly reduced. The tumour inhibition rate after treatment was significantly higher, and throughout the treatment process, CyMe-Pt exhibited a higher photothermal conversion efficiency (37%) and better biological stability. Compared to J-aggregates, H-aggregates may have a more significant impact on enhancing the efficiency of light-to-heat conversion. In 2024,[123] Yang and his team designed a photothermal agent based on cyanine dyes, namely, poly(dopamine)-coated H-aggregates (Cy-aggregate@PDA) (Figure 10E). The study used cyanine dyes with zwitterionic charges, which formed H-aggregates with significant NIR absorption through charge interactions and π-π interactions. The researchers then coated these dye aggregates with poly-dopamine to create a core-shell structured nanomaterial. This innovative strategy improved the photostability and thermal stability of the dye aggregates and significantly increased the photothermal conversion efficiency. The study showed that the photothermal conversion


https://doi.org/10.2147/IJN.S542880

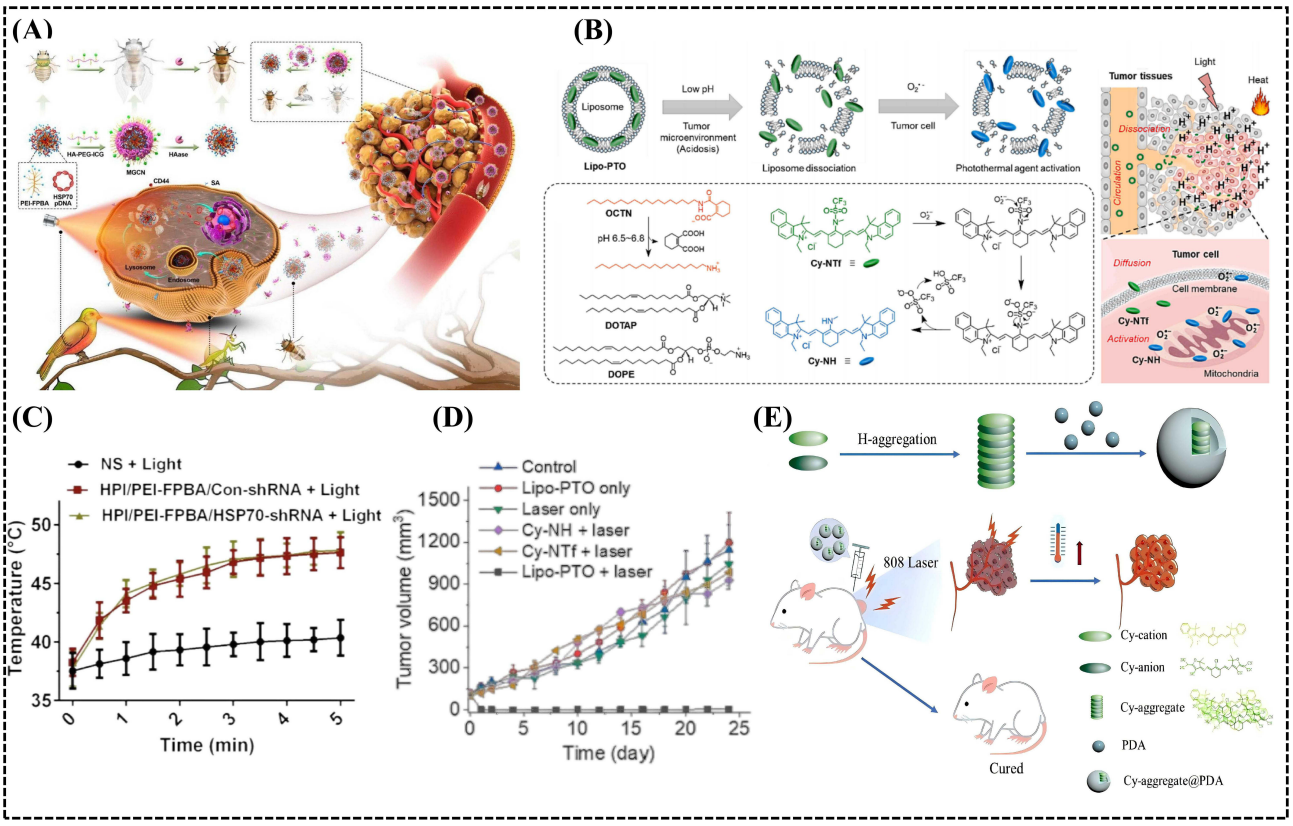


**Figure 10** (**A**) Schematic of a multifunctional Golden Cicada nanoplatform for cancer therapy. Reproduced from Yang W, Wang N, Yang J et al. A multifunctional "golden cicada" nanoplatform breaks the thermoresistance barrier to launch cascade augmented synergistic effects of photothermal/gene therapy. J Nanobiotechnology, 2023, 21:228. Creative Commons Attribution 4.0 International License.[118] (**B**) Schematic representation of the synthesis and application of Lipo-PTO nanoprobes. Reproduced from Wang W, Zhang Y, Zhang Y et al. Biomimetic liposomes as a pH/ROS cascade-responsive nanoagent with high selectivity for breast carcinoma in photothermal therapy. Mater Des, 2023, 234:112304. © 2023 The Authors. Published by Elsevier Ltd. This is an open access article under the CC BY-NC-ND license.[121] (**C**) Temperature rise curve of tumour-bearing mice after 5 minutes of irradiation. Reproduced from Yang W, Wang N, Yang J et al. A multifunctional "golden cicada" nanoplatform breaks the thermoresistance barrier to launch cascade augmented synergistic effects of photothermal/gene therapy. J Nanobiotechnology, 2023, 21:228. Creative Commons Attribution 4.0 International License. Creative Commons Attribution 4.0 International License.[118] (**D**) Quantification of treatment effects in different groups of mice. Reproduced from Wang W, Zhang Y, Zhang Y et al. Biomimetic liposomes as a pH/ROS cascade-responsive nanoagent with high selectivity for breast carcinoma in photothermal therapy. Mater Des, 2023, 234:112304. © 2023 The Authors. Published by Elsevier Ltd. This is an open access article under the CC BY-NC-ND license.[121] (**E**) Schematic of Cy-aggregate @PDA photothermal imaging and therapy. Reproduced from Yang H, Yuan W, Cao J et al. Poly(dopamine) coated H-aggregates of amphoteric charged near-infrared absorbing cyanine dyes for enhanced photothermal tumor imaging and therapy. Dyes Pigm, 2024, 226:112141. *© 2024 Elsevier Ltd. All rights reserved.*[123]

efficiency of Cy-aggregate@PDA reached 51.4%. In in vitro experiments, Cy-aggregate@PDA reached a maximum temperature of 54°C under 808 nm laser irradiation, demonstrating excellent photothermal effect and stability. In an in vivo experiment using a mouse tumour model, the temperature in the tumour area rose rapidly to 58.2°C after injection of Cy-aggregate@PDA, which was significantly higher than the 35°C in the control group. After 15 days of treatment, the tumour volume in the Cy-aggregate@PDA group was significantly reduced to one fifth of the initial volume, while the tumours in the cyanine aggregate treatment group without coated polydopamine continued to grow. These nanoprobe platforms leverage the unique photothermal properties of cyanine dyes, demonstrating remarkable efficacy in photothermal cancer therapy. When integrated with various biocompatible materials, they exhibit excellent biocompatibility, providing strong support for efficient and safe tumor ablation. However, due to the limited penetration depth of NIR laser, further research and optimization are required for the treatment of deeper tumors.

## Combined Treatment of PTT and PDT in Tumours with Cyanine Nanprobes

The treatment of tumours with PTT/PDT alone is not very effective. In 2013,[124] Kim et al tested the effectiveness of PDT alone, PTT alone and a combination of PTT and PDT in the treatment of squamous cell carcinoma. PDT alone was initially effective, but the tumour began to grow rapidly again after 7 days. Treatment with PTT alone was more effective than treatment with PDT, but it could only suppress tumour growth for 10 days, after which the tumour began to grow again. The

combined treatment with PTT and PDT was the most effective, with no recurrence during the 15-day observation period. Therefore, the development and application of combined PDT/PTT therapy are increasingly significant and effective. In 2023,[125] Tianguang Liu et al developed a photothermal inhibitor based on nonionic heptamethine cyanine dye for synergistic cancer phototherapy, particularly combining PDT and PTT (Figure 11A). They introduced carboxyl or sulfonic groups into the indole ring of heptamethine cyanine to create BSS-Et nanoprobes. These nanoprobes exhibited excellent photostability and efficient ROS generation (up to 49%), achieving a photothermal conversion efficiency of approximately 37.6% under 808 nm laser irradiation. The experimental results showed that in the BSS-Et NPs + laser treatment group, the 4T1 solid tumors in mice almost completely disappeared without recurrence after 19 days of treatment, although slight burn scars were observed at the tumor site, which gradually healed within a few days. This strongly demonstrates the remarkable in vivo antitumor effect of BSS-Et NPs through the synergistic action of PTT and PDT. In 2023,[126] Yu Li et al also developed an "all-in-one" heptamethine cyanine amphiphilic compound platform named PEG-Cy-F18 (Figure 11B). These amphiphiles exhibited PDT and PTT therapeutic effects as well as PEGylated biocompatibility. The self-assembled nanoprobes showed high PDT and PTT efficiency, with a significant temperature increase under 750 nm laser irradiation. Notably, the study achieved a PCE of approximately 22% for PEG-Cy-F18, which was higher than that of the base IR780 dye. In an MCF-7 human breast cancer model, the nanoprobes demonstrated a high therapeutic effect, with complete tumor ablation achieved in all five mice subjected to laser treatment. This also reflected the exceptional in vivo antitumor efficacy of the combined PTT and PDT therapy. In same year,[127] Xiangtan University developed a tumour-targeted fluorescent probe called Cy-Bio -O, which targets tumours by introducing a biotin structure into the probe (Figure 11C). This probe can activate its PDT and PTT functions simultaneously under acidic conditions. Studies have shown that Cy-Bio-O exhibits significant PTT effects in in vitro experiments. Under 660 nm laser irradiation, the temperature can rise rapidly from 24.6°C to 82.4°C, indicating its excellent PTT properties. In terms of PDT, Cy-Bio-O can produce ROS under acidic conditions, and its PDT properties have been confirmed in cell experiments by in vivo imaging. In vivo experiments have shown that this probe can achieve efficient imaging and treatment of tumours in tumour-bearing mice, significantly inhibiting tumour growth. Under the synergistic effect of PDT therapy and PTT therapy, the tumour shrinks by 70%, indicating that it has significant anti-tumour effects in the synergistic treatment of PDT/PTT dual modes. In 2024,[128] Yu and his team designed a smart photosensitizer Cy5-TPA based on anthraquinone dyes, which optimises its PDT and PTT properties by introducing a triphenylamine (TPA) group. The introduction of TPA enhances intramolecular charge transfer (ICT), which improves the photosensitizer's ROS generation capacity at low temperatures, while enhancing photothermal conversion at high temperatures. This characteristic enables Cy5-TPA to adaptively switch from PDT-dominant to PTT-dominant during temperature changes at the tumour site, thereby maximising the phototherapy effect. Studies have shown that Cy5-TPA exhibits high ROS generation at low temperatures (25°C), while at higher temperatures (45°C) it exhibits stronger photothermal conversion (photothermal conversion efficiency up to 45.6%). In addition, the design of Cy5-TPA not only improves the ROS generation capacity, but also significantly enhances its photothermal stability and phototherapy efficiency. Cy5-TPA can photothermally kill tumour cells in vitro, and significantly inhibit tumours and enhance anti-tumour immunity in vivo through switching between PDT and PTT. Above all, these studies have demonstrated the effectiveness of PTT and PDT in tumor therapy by introducing multifunctional formulations based on cyanine dyes, improving photothermal conversion, and combining multimodal imaging to achieve more precise and beneficial therapeutic outcomes. In another study, Professor Dong's team[129] developed a photo-activated nanozyme (IR/P@Ce) composed of the photosensitizer IR820, polydopamine (PDA), and mesoporous cerium dioxide ($mCeO_2$) (Figure 11D). Through the bridging effect of PDA, efficient electron transfer between IR820 and $mCeO_2$ was achieved, which significantly enhanced the peroxidase (POD)-like catalytic activity and reactive ROS generation. Moreover, PDA not only improved the structural stability of the nanozyme and the efficacy of PDT, but also markedly boosted the performance of PTT. The development of multifunctional platforms based on cyanine dyes has enhanced the efficacy of PDT and PTT. However, further research is needed to optimize these methods for deeper tumors and improve long-term treatment outcomes.

## Synergistic Strategies of PTT/PDT to Enhance Other Cancer Therapies

At present, in addition to the direct use of PTT and PDT for cancer treatment, combining these modalities with other conventional and newly discovered therapeutic strategies has gained significant attention. Specifically, the integration of

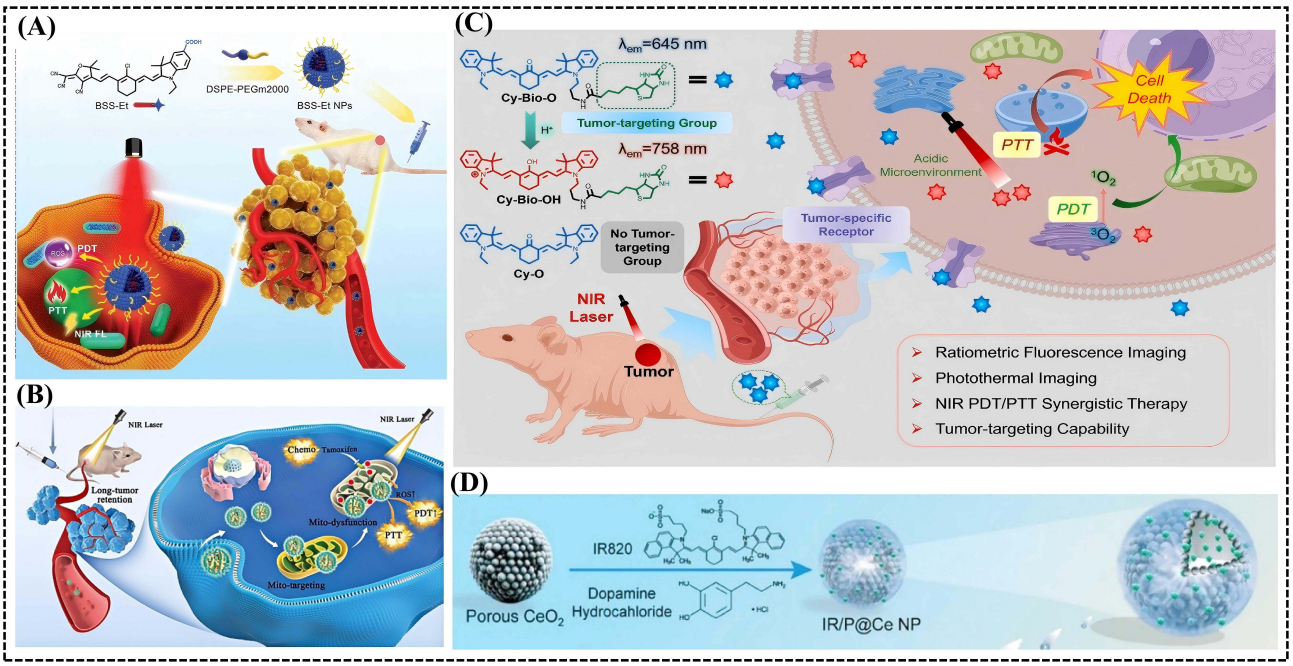


**Figure 11** (**A**) Schematic representation of the molecular structure and properties of phototherapeutic agents of BSS-Et NPs. Reproduced from Liu T, Chen Y, Wang H et al. Phototheranostic agents based on nonionic heptamethine cyanine for realizing synergistic cancer phototherapy. Adv Healthc Mater, 2023, 12:2202817. © 2023 Wiley-VCH GmbH.[125] (**B**) Schematic of SoFoTm/PEG-Cy-F18 nanoparticle synthesis and chemo-PTT-PDT combination therapy for breast cancer. Reproduced from Li Y, Zhang J, Zhu L et al. All-in-one heptamethine cyanine amphiphiles for dual imaging-guided chemo-photodynamic-photothermal therapy of breast cancer. Adv Healthc Mater, 2023, 12:2300941. © *2023 Wiley-VCH GmbH.*[126] (**C**) Chemical structure and biological applications of the probe Cy-Bio-O. Reproduced from Gu QS, Li T, Wang WX et al. A tumor-targeting fluorescent probe for ratiometric imaging of pH and improving PDT/PTT synergistic therapy. Sens Actuators B Chem, 2023, 393:134287. Copyright 2023, Elsevier BV.[127] (**D**) Schematic representation of the synthesis of IR/P@Ce NPs. Reproduced from Juaim AN, Sun J, Nie R, Alruwaili NK, Al-Kattan WM, Aldosari B et al. IR820 sensitized ceria nanozyme via PDA bridging for multifaceted antibacterial wound healing therapy. Small, 2025, 21:2500382. © *2025 Wiley-VCH GmbH.*[129]

cyanine dyes in PTT and PDT therapies with chemotherapy and immune therapy has shown promising results. For chemotherapy, Kathryn M. and others[130] investigated the strategy of combining cyanine dyes with the chemotherapy drug Crizotinib to enhance the therapeutic effect. Crizotinib is a chemotherapy drug with clinical potential for the treatment of glioblastoma.[131] They developed a novel conjugate form of the cyanine dye IR786 and Crizotinib (IR-Crizotinib) and found that this conjugate can significantly increase the targeting and accumulation of Crizotinib in brain tumours and improve the efficiency of the drug crossing the blood-brain barrier. In treatment experiments, IR-Crizotinib showed stronger tumour growth inhibition and higher levels of tumour cell apoptosis than Crizotinib alone or the IR786 dye. After 4 weeks of treatment, mice in the IR-Crizotinib group showed smaller, localised tumours, while the Crizotinib alone or untreated groups showed larger and more intensive tumour growth. In 2024,[132] Chen et al explored the use of mild hyperthermia phototherapy PTT triggered by NIR light in combination with the chemotherapeutic drug cisplatin to overcome drug resistance in cancer (Figure 12A). Cisplatin is a widely used chemotherapeutic drug that kills cancer cells by forming crosslinks with their DNA, inhibiting replication and division.[133] The research team designed a self-assembled nanoagent (Cy-Pt@HA NPs) that combines the anthracene dye cypate, the Pt(IV) prodrug and $Gd^{3+}$ ions, and is surface-modified with hyaluronic acid (HA) to enhance tumour targeting. In treatment experiments, Cy-Pt@HA NPs can heat the tumour area to about 43 °C under 785 nm laser irradiation, thereby significantly increasing drug uptake and cell membrane permeability. The experimental results show that compared with the non-irradiated group, NIR light irradiation of Cy-Pt@HA NPs significantly enhances the formation of Pt-DNA adducts, overcomes the drug tolerance of cisplatin, and shows excellent anti-tumor effects in the A549R drug-resistant tumor model. Specific data show that the tumour inhibition rate in the Cy-Pt@HA NPs group reached 91%, while cell viability decreased to 8.9% after treatment with high concentrations of Pt, indicating that this strategy has significant advantages in overcoming drug resistance.

For immune therapy, in 2023,[134] Wang et al investigated the use of mitochondrial-targeted PDT and mild PTT in combination with immunotherapy to enhance the efficacy of tumour treatment (Figure 12B). The research team

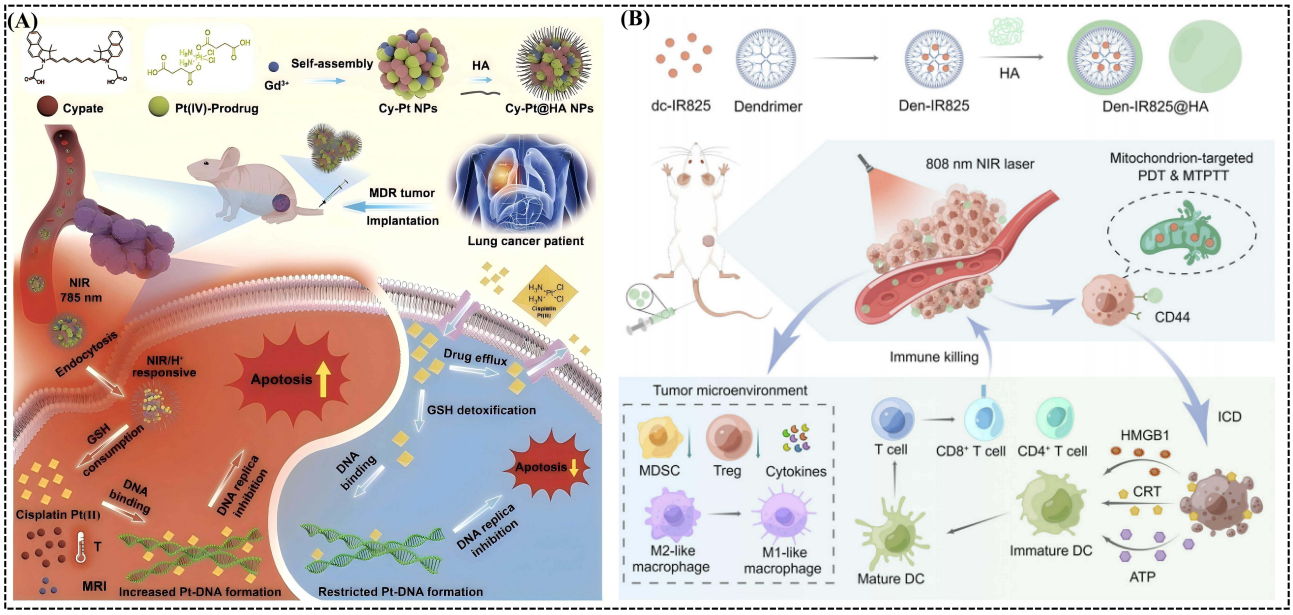


**Figure 12** (**A**) Schematic representation of the synthesis of Cy-Pt@HA nanoparticles and the achievement of mild photothermal chemotherapy (yellow upward arrow indicates an increase in apoptosis) (yellow downward arrow indicates a decrease in apoptosis). Reproduced from Chen M, Fu Y, Liu Y et al. NIR-light-triggered mild-temperature hyperthermia to overcome the cascade cisplatin resistance for improved resistant tumor therapy. Adv Healthc Mater, 2024, 13:2303667. © *2024 Wiley-VCH GmbH.*[132] (**B**) Fabrication of DIH and its application in mitochondria-targeted PDT/MTPTT and ICD induction via mitochondrial stress–mediated immunostimulation. Reproduced from Wang SZ, Guo Y, Zhang X, Zhao Y, Wang R, Xu Y et al. Mitochondria-targeted photodynamic and mild-temperature photothermal therapy for realizing enhanced immunogenic cancer cell death via mitochondrial stress. Adv Funct Mater, 2023, 33:2303328. © 2023 Wiley-VCH.[134]

developed a polyamide-amine dendrimer (PAMAM)-based nanoparticle platform DIH, which contains the mitochondrial-targeted anthracene dye dc-IR825 and is modified with HA to improve tumour uptake and targeting. The DIH nanoplatform is capable of generating ROS and mild heat upon NIR light (808 nm) irradiation, which triggers mitochondrial damage and induces enhanced immunogenic cell death (ICD). In vivo experiments, the temperature in the tumour region of mice treated with DIH and light rose to 44.1°C. Compared with the control group, DIH treatment significantly inhibited tumour growth, with complete regression observed in some mice, and promoted immune activation (upregulation of CRT and ATP release, DC maturation), increased CD4+/CD8+ T cell and M1 macrophage infiltration, and reduced M2 macrophage and Treg numbers. This combined treatment strategy effectively activated the anti-tumour immune response. In 2024,[135] Yu et al designed and developed a cyanidin immunomodulator $I_2$HCy-QAP that targets mitochondria, and combined it with an antiprogrammed death-1 antibody, for combination therapy. $I_2$HCy-QAP enhances $^1O_2$ production by introducing an iodine-containing structure, and enables high-contrast visualization of tumors by NIR-II fluorescence imaging. Experimental data show that $I_2$HCy-QAP has a $^1O_2$ quantum yield of up to 27.4% under laser irradiation. In vivo experiments showed that $I_2$HCy-QAP combined with PDT and αPD-1 antibody treatment significantly inhibited primary and distant metastatic tumours in a triple-negative breast cancer model, with a 100% inhibition rate in primary tumours and a significant reduction in the formation of lung metastases. In addition, in the combination therapy group, the maturation rate of splenic dendritic cells (DCs) in mice was 18.0%, which was significantly higher than that in the single therapy group, and the infiltration rate of CD8+ T cells was also significantly increased, showing a strong anti-tumor immune response and superior therapeutic effect. These nanoprobes have demonstrated significant synergistic effects in the combined strategy of phototherapy and immunotherapy for cancer, advancing the development of precision treatment and systemic anti-tumor immunity. The combination of PTT, PDT, and conventional therapies shows promising results in cancer treatment, but challenges remain in optimizing these approaches for deep tumors and consistent immune responses. Further refinement is needed for broader clinical application.

## Discussion

Current cyanine based nanoprobes, despite ongoing advancements and developments, still face numerous challenges. In terms of imaging, the first issue is their poor performance in long-term imaging applications, particularly in deep tissue imaging. Secondly, cyanine dye-based nanoprobes face multiple challenges in achieving long-term detection within biological systems. They are easily metabolised and cleared from the body, and they are prone to photobleaching during illumination, leading to significantly reduced retention time within the body and degraded imaging performance. Additionally, when combined with other biomolecules, cyanine nanoprobes may interact with them, resulting in structural instability.

In terms of therapy, some cyanine-based nanoprobes exhibit low efficiency in PTT and PDT, failing to generate sufficient heat or ROS, thereby limiting their efficacy in these treatments. Furthermore, the sensitivity and specificity of cyanine-based nanoprobes across different diseases or different subtypes of the same disease require further improvement. For example, different types of tumour cells may have different surface markers, requiring nanoprobes to precisely identify these differences. For different subtypes of the same disease, due to minor differences in molecular characteristics, existing cyanide-based nanoprobes may be unable to effectively distinguish between them or may lack sufficient sensitivity for certain subtypes.

The clinical translation of cyanine-based nanoprobes faces major challenges, notably stringent regulatory requirements that may delay market approval, particularly for nanomaterials. Scaling up clinical-grade production is hindered by complex synthesis and quality control demands. Furthermore, discrepancies in metabolism, immune responses, and anatomy between animal models and humans limit the predictive value of preclinical studies. Overcoming these barriers requires improving diagnostic and therapeutic technologies to enhance sensitivity and specificity, and adopting more human-relevant models to strengthen translational accuracy.

## Summary and Outlook

In recent years, the development of cyanine dye-based nanoprobes for integrated tumor diagnosis and therapy has attracted increasing attention. Over the past four to five years, numerous research groups have designed various NIR responsive cyanine nanoprobes to overcome the limitations of conventional tumor diagnostic and therapeutic methods. However, despite these promising developments, several challenges must be addressed to further expand the clinical application of NIR cyanine nanoprobes: (1) Low and unstable fluorescence quantum yield. (2) Limited long-term detection capability in vivo. (3) Limited therapeutic efficacy in NIR PTT and PDT. (4) Poor adaptability to different diseases or subtypes. Therefore, future research should focus on improving the fluorescence quantum yield and stability of cyanine dyes, optimising their long-term detection capabilities in vivo, and enhancing the therapeutic effects of photothermal and photodynamic therapies. Through multifunctional design, cyanine nanoprobes should be able to adapt to different diseases or subtypes, driving the application of personalised medicine. During the clinical translation process, issues such as the probe's biocompatibility, tissue permeability, and biodegradability must also be addressed to ensure its safety and efficacy in clinical settings. Moreover, an engineering-biology-clinical medicine consortium should be established to facilitate the broader application and clinical translation of NIR cyanine fluorescent probes.[136]

## Acknowledgments

This work was supported by the key Project of Xinjiang Uygur Autonomous Region Natural Science Foundation Youth Top Talent Project (No. 2022TSYCCX0032), Xinjiang Uygur Autonomous Region Natural Science Foundation (No. 2022D01D40), Xinjiang Uygur Autonomous Region Regional Collaborative Innovation Special Science and Technology Assistance Program (No. 2022E02130), the National Natural Science Foundation of China (NSFC) under Grant (Program No. 62035011, No.82202220, No. 82073475, No. 52250007 and No. 82060326), Xinjiang Uygur Autonomous Region Natural Science Foundation Outstanding Youth Project (No. 2023D01E06), Tianchi Talent Project (03010511), State Key Laboratory of Pathogenesis, Prevention and treatment of High Incident Diseases in central Asia (SKLHIDCA-2024-GJ9).

## Disclosure

The authors declare that they have no known competing financial interests or personal relationships that could have appeared to influence the work reported in this paper.

## References


1. Liu B, Zhou H, Tan L, et al. Exploring treatment options in cancer: tumor treatment strategies. *Signal Transduct Target Ther*. 2024;9:175. doi:10.48550/arXiv.2411.02843
2. Chan YT, Zhang C, Wu J, et al. Biomarkers for diagnosis and therapeutic options in hepatocellular carcinoma. *Mol Cancer*. 2024;23:189. doi:10.1186/s12943-024-02101-z
3. Kumar A, Dubey US, Dubey B. The impact of radio-chemotherapy on tumour cells interaction with optimal control and sensitivity analysis. *Math Biosci*. 2024;369:109146. doi:10.1016/j.mbs.2024.109146
4. Yang Z, Liu X, Xu H, et al. Integrative analysis of genomic and epigenomic regulation reveals miRNA mediated tumor heterogeneity and immune evasion in lower grade glioma. *Commun Biol*. 2024;7(1):824. doi:10.1038/s42003-024-06488-9
5. Park J, Choi S, Knieling F, et al. Clinical translation of photoacoustic imaging. *Nat Rev Bioeng*. 2024;3:1–20. doi:10.1038/s44222-024-00240-y
6. Richards-Kortum R, Lorenzoni C, Bagnato VS, et al. Optical imaging for screening and early cancer diagnosis in low-resource settings. *Nat Rev Bioeng*. 2024;2:25–43. doi:10.1038/s44222-023-00135-4
7. Yamamoto H. Micrometastasis in lymph nodes of colorectal cancer. *Ann Gastroenterol Surg*. 2022;6:466–473. doi:10.1002/ags3.12576
8. Ma S, Sun B, Li M, et al. High-precision detection and navigation surgery of colorectal cancer micrometastases. *J Nanobiotechnology*. 2023;21:403. doi:10.1186/s12951-023-02171-z
9. Lee DE, Koo H, Sun IC, et al. Multifunctional nanoparticles for multimodal imaging and theragnosis. *Chem Soc Rev*. 2012;41:2656–2672. doi:10.1039/C2CS15261D
10. Ji Y, Jones C, Baek Y, et al. Near-infrared fluorescence imaging in immunotherapy. *Adv Drug Deliv Rev*. 2020;167:121–134. doi:10.1016/j.addr.2020.06.012
11. Josserand V, Kéramidas M, Lavaud J, et al. Electrochemotherapy guided by intraoperative fluorescence imaging for the treatment of inoperable peritoneal micro-metastases. *J Control Release*. 2016;233:81–87. doi:10.1016/j.jconrel.2016.05.003
12. Hilderbrand SA, Weissleder R. Near-infrared fluorescence: application to in vivo molecular imaging. *Curr Opin Chem Biol*. 2010;14:71–79. doi:10.1016/j.cbpa.2009.09.029
13. Al-Thani AN, Jan AG, Abbas M, et al. Nanoparticles in cancer theragnostic and drug delivery: a comprehensive review. *Life Sci*. 2024;352:122899. doi:10.1016/j.lfs.2024.122899
14. Taha BA, Kadhim AC, Addie AJ, et al. Advancing cancer diagnostics through multifaceted optical biosensors supported by nanomaterials and artificial intelligence: a panoramic outlook. *Microchem J*. 2024;205:111307. doi:10.1016/j.microc.2024.111307
15. Nag S, Mitra O, Tripathi G, et al. Nanomaterials-assisted photothermal therapy for breast cancer: state-of-the-advances and future perspectives. *Photodiagnosis Photodyn Ther*. 2024;45:103959. doi:10.1016/j.pdpdt.2023.103959
16. Yang RQ, Lou KL, Wang PY, et al. Surgical navigation for malignancies guided by near-infrared-II fluorescence imaging. *Small Methods*. 2021;5(3):2001066. doi:10.1002/smtd.202001066
17. Tobias JD. Cerebral oxygenation monitoring: near-infrared spectroscopy. *Expert Rev Med Devices*. 2006;3(2):235–243. doi:10.1586/17434440.3.2.235
18. Liu Z, Si L, Shi S, et al. Classification of three anesthesia stages based on near-infrared spectroscopy signals. *IEEE J Biomed Health Inform*. 2024;28(9):5270–5279. doi:10.1109/JBHI.2024.3409163
19. Liu W, Zhang Y, Qi J, Qian J, Tang BZ. NIR-II excitation and NIR-I emission based two-photon fluorescence lifetime microscopic imaging using aggregation-induced emission dots. *Chem Res Chin Univ*. 2021;37:171–176. doi:10.1007/s40242-021-0405-2
20. Chen ZH, Wang X, Yang M, et al. An extended NIR-II superior imaging window from 1500 to 1900 nm for high-resolution in vivo multiplexed imaging based on lanthanide nanocrystals. *Angew Chem*. 2023;135:e202311883. doi:10.1002/ange.202311883
21. Vitorino R, Barros AS, Guedes S, et al. Diagnostic and monitoring applications using near infrared (NIR) spectroscopy in cancer and other diseases. *Photodiagnosis Photodyn Ther*. 2023;42:103633. doi:10.1016/j.pdpdt.2023.103633
22. Li M, Zheng X, Han T, et al. Near-infrared-II ratiometric fluorescence probes for non-invasive detection and precise navigation surgery of metastatic sentinel lymph nodes. *Theranostics*. 2022;12:7191. doi:10.7150/thno.78085
23. Heinz MC, Peters NA, Oost KC, et al. Liver colonization by colorectal cancer metastases requires YAP-controlled plasticity at the micrometastatic stage. *Cancer Res*. 2022;82:1953–1968. doi:10.1158/0008-5472.CAN-21-0933
24. Zhou HJ, Ren TB. Recent progress of cyanine fluorophores for NIR-II sensing and imaging. *Chem Asian J*. 2022;17:e202200147. doi:10.1002/asia.202200147
25. Sharma M, Alessandro P, Cheriyamundath S, Lopus M. Therapeutic and diagnostic applications of carbon nanotubes in cancer: recent advances and challenges. *J Drug Target*. 2024;32:287–299. doi:10.1080/1061186X.2024.2309575
26. Li H, Du Z, Zhu L, et al. Ultrabright NIR-IIb fluorescence quantum dots for targeted imaging-guided surgery. *ACS Appl Mater Interfaces*. 2024;16:32045–57 doi:10.1021/acsami.4c04748..
27. Li J, Chang X, Chen X, et al. Toxicity of inorganic nanomaterials in biomedical imaging. *Biotechnol Adv*. 2014;32:727–743. doi:10.1016/j.biotechadv.2013.12.009
28. Wu J, Shi Z, Zhu L, et al. The design and bioimaging applications of NIR fluorescent organic dyes with high brightness. *Adv Opt Mater*. 2022;10:2102514. doi:10.1002/adom.202102514
29. Yang Y, Gao F, Wang Y, et al. Fluorescent organic small molecule probes for bioimaging and detection applications. *Molecules*. 2022;27:8421. doi:10.3390/molecules27238421
30. Su Y, Yu B, Wang S, et al. NIR-II bioimaging of small organic molecule. *Biomaterials*. 2021;271:120717. doi:10.1016/j.biomaterials.2021.120717
31. Tian R, Feng X, Wei L, et al. A genetic engineering strategy for editing near-infrared-II fluorophores. *Nat Commun*. 2022;13:2853. doi:10.1038/s41467-022-30304-9

32. Wang D, Yue J, Cao Q, et al. ICG-loaded and 125I-labeled theranostic nanosystem for multimodality imaging-navigated phototherapy of breast cancer. *Biomater Sci*. 2023;11:248–262. doi:10.1039/D2BM01551J
33. Nagy BI, Mohos B, Tzou CHJ. Imaging modalities for evaluating lymphedema. *Medicina*. 2023;59:2016. doi:10.3390/medicina59112016
34. Li Q, Chen K, Huang W, et al. Minimally invasive photothermal ablation assisted by laparoscopy as an effective preoperative neoadjuvant treatment for orthotopic hepatocellular carcinoma. *Cancer Lett*. 2021;496:169–178. doi:10.1016/j.canlet.2020.09.024
35. Ren H, Zeng XZ, Zhao XX, et al. A bioactivated in vivo assembly nanotechnology fabricated NIR probe for small pancreatic tumor intraoperative imaging. *Nat Commun*. 2022;13:418. doi:10.1038/s41467-021-27932-y
36. Du Z, Ma R, Chen S, et al. A highly efficient polydopamine encapsulated clinical ICG theranostic nanoplatform for enhanced photothermal therapy of cervical cancer. *Nanoscale Adv*. 2022;4:4016–4024. doi:10.1039/D2NA00341D
37. Li Y, Yi M, Xiong B, et al. pH-responsive degradable mesoporous organosilica nanoparticle for tumor targeting and phototherapy combined with chemotherapy. *J Drug Deliv Sci Technol*. 2024;92:105344. doi:10.1016/j.jddst.2024.105344
38. Zhou Y, Jiang G, Wang W, et al. A novel near-infrared fluorescent probe TMTP1-PEG4-ICG for in vivo tumor imaging. *Bioconjug Chem*. 2018;29(12):4119–4126. doi:10.1021/acs.bioconjchem.8b00756
39. Jiang G, Wang X, Zhou Y, et al. TMTP1-modified, tumor microenvironment responsive nanoparticles co-deliver cisplatin and paclitaxel prodrugs for effective cervical cancer therapy. *Int J Nanomedicine*. 2021;16:4087–4104. doi:10.2147/IJN.S298252
40. Qiu Y, Yuan B, Cao Y, et al. Recent progress on near-infrared fluorescence heptamethine cyanine dye-based molecules and nanoparticles for tumor imaging and treatment. *Wiley Interdiscip Rev Nanomed Nanobiotechnol*. 2023;15(5):e1910. doi:10.1002/wnan.1910
41. Xu L, Zhang Q, Wang X, Lin W. Biomedical applications of NIR-II organic small molecule fluorescent probes in different organs. *Coord Chem Rev*. 2024;519:216122. doi:10.1016/j.ccr.2024.216122
42. Zheng J, Chen SH, Huang B, Zhang M, Yuan Q, Cui R. Imaging-guided precision oncotherapy mediated by nanoprobes: from seeing to curing. *Chin Chem Lett*. 2024;35:108460. doi:10.1016/j.cclet.2023.108460
43. An Q, Xiang SR, Zou YQ. Recent progresses in combination cancer therapy using cyanine dye-based nanoparticles. *Pharm Sci Adv*. 2024;100040. doi:10.1016/j.pscia.2024.100040
44. Sun W, Guo S, Hu C, Fan J, Peng X. Recent development of chemosensors based on cyanine platforms. *Chem Rev*. 2016;116(14):7768–7817. doi:10.1021/acs.chemrev.6b00001
45. Shindy HA. Fundamentals in the chemistry of cyanine dyes: a review. *Dyes Pigm*. 2017;145:505–513. doi:10.1016/j.dyepig.2017.06.029
46. Medeiros NG, Braga CA, Câmara VS, Duarte RC, Rodembusch FS. Near-infrared fluorophores based on heptamethine cyanine dyes: from their synthesis and photophysical properties to recent optical sensing and bioimaging applications. *Asian J Org Chem*. 2022;11:e202200095. doi:10.1002/ajoc.202200095
47. Dar N, Ankari R. Theoretical models, preparation, characterization and applications of cyanine J-aggregates: a minireview. *ChemistryOpen*. 2022;11:e202200103. doi:10.1002/open.202200103
48. Delaey E, van Laar F, De Vos D, Kamuhabwa A, Jacobs P, de Witte P. A comparative study of the photosensitizing characteristics of some cyanine dyes. *J Photochem Photobiol B*. 2000;55(1):27–36. doi:10.1016/S1011-1344(00)00021-X
49. Abeywickrama CS. Large Stokes shift benzothiazolium cyanine dyes with improved intramolecular charge transfer (ICT) for cell imaging applications. *Chem Commun*. 2022;58:9855–9869. doi:10.1039/D2CC03880C
50. Williams CG. XXVI.—researches on chinoline and its homologues. *Earth Environ Sci Trans R Soc Edinb*. 1857;21:377–401. doi:10.1017/S0080456800032208
51. Brooker LG. The cyanine dyes and related compounds. *J Am Chem Soc*. 1965;87:937–938. doi:10.1021/ja01082a060
52. Ilina K, Henary M. Cyanine dyes containing quinoline moieties: history, synthesis, optical properties, and applications. *Chem Eur J*. 2021;27:4230–4248. doi:10.1002/chem.202003697
53. Zhang C, Long L, Shi C. Mitochondria-targeting IR-780 dye and its derivatives: synthesis, mechanisms of action, and theranostic applications. *Adv Ther*. 2018;1:1800069. doi:10.1002/adtp.201800069
54. Cooksey CJ. Abbreviations for dyes, stains and fluorescent probes used in biology and medicine in the 21st century: a bright future or the last gasp? *Biotech Histochem*. 2021;96:401–407. doi:10.1080/10520295.2021.1897677
55. Ernst LA, Gupta RK, Mujumdar RB, Waggoner AS. Cyanine dye labeling reagents for sulfhydryl groups. *Cytometry*. 1989;10:3–10. doi:10.1002/cyto.990100103
56. Zhang J, Chen X, Liu J, et al. Non-small nanoprobes based on FDA-approval formulation for NIR-II imaging and detection of drug-induced acute kidney injury. *Dyes Pigm*. 2025;235:112598. doi:10.1016/j.dyepig.2024.112598
57. Zhu S, Tian R, Antaris AL, et al. Near-infrared-II molecular dyes for cancer imaging and surgery. *Adv Mater*. 2019;31:1900321. doi:10.1002/adma.201900321
58. Zhu L, Du Z, Xiong J, et al. Phototheranostic LPP-QDs-IR-820 nanocomposites for specific NIR-II imaging of lymphatic and photothermal therapy of cervical tumors. *Adv Healthc Mater*. 2024;13:2401358. doi:10.1002/adhm.202401358
59. Bar N, Chowdhury P. A brief review on advances in rhodamine B based chromic materials and their prospects. *ACS Appl Electron Mater*. 2022;4:3749–3771. doi:10.1021/acsaelm.2c00107
60. Jiang G, Hu Z, Bai L, et al. Origins of near-infrared-II emission tail and fluorescence enhancement of albumin-chaperoned cyanine dyes from a multiscale computational study. *J Mater Chem C*. 2023;11:7243–7251. doi:10.1039/D3TC00452J
61. Hestand NJ, Spano FC. Expanded theory of H- and J-molecular aggregates: the effects of vibronic coupling and intermolecular charge transfer. *Chem Rev*. 2018;118:7069–7163. doi:10.1021/acs.chemrev.7b00581
62. Sun C, Li B, Zhao M, et al. J-aggregates of cyanine dye for NIR-II in vivo dynamic vascular imaging beyond 1500 nm. *J Am Chem Soc*. 2019;141:19221–19225. doi:10.1021/jacs.9b10043
63. Kawelah MR, Han S, Atila Dincer C, et al. Antibody-conjugated polymersomes with encapsulated indocyanine green J-aggregates and high near-infrared absorption for molecular photoacoustic cancer imaging. *ACS Appl Mater Interfaces*. 2024;16:5598–5612. doi:10.1021/acsami.3c16584
64. Li M, Sun W, Tian R, et al. Smart J-aggregate of cyanine photosensitizer with the ability to target tumor and enhance photodynamic therapy efficacy. *Biomaterials*. 2021;269:120532. doi:10.1016/j.biomaterials.2020.120532

65. Wu F, Lu Y, Mu X, et al. Intriguing H-aggregates of heptamethine cyanine for imaging-guided photothermal cancer therapy. *ACS Appl Mater Interfaces*. 2020;12:32388–32396. doi:10.1021/acsami.0c07608
66. Lei Z, Sun C, Pei P, et al. Stable, wavelength-tunable fluorescent dyes in the NIR-II region for in vivo high-contrast bioimaging and multiplexed biosensing. *Angew Chem*. 2019;131:8250–8255. doi:10.1002/ange.201904182
67. Bouit PA, Aronica C, Toupet L, Le Guennic B, Andraud C, Maury O. Continuous symmetry breaking induced by ion pairing effect in heptamethine cyanine dyes: beyond the cyanine limit. *J Am Chem Soc*. 2010;132:4328–4335. doi:10.1021/ja9100886
68. Yu J, Rong J, Yuan S, et al. Extending the emission peak tail of indole cyanine for deep-near-infrared bioimaging. *Spectrochim Acta A Mol Biomol Spectrosc*. 2024;322:124798. doi:10.1016/j.saa.2024.124798
69. Awasthi K, Nishimura G. Modification of near-infrared cyanine dyes by serum albumin protein. *Photochem Photobiol Sci*. 2011;10:461–463. doi:10.1039/c0pp00271b
70. Patonay G, Kim JS, Kodagahally R, Strekowski L, Thompson R, Pappas TN. Spectroscopic study of a novel bis(heptamethine cyanine) dye and its interaction with human serum albumin. *Appl Spectrosc*. 2005;59:682–690. doi:10.1366/0003702053945976
71. Bai L, Hu Z, Han T, et al. Super-stable cyanine@albumin fluorophore for enhanced NIR-II bioimaging. *Theranostics*. 2022;12:4536. doi:10.7150/thno.71443
72. Du B, Qu C, Qian K, et al. An IR820 dye–protein complex for second near-infrared window and photoacoustic imaging. *Adv Opt Mater*. 2020;8:1901471. doi:10.1002/adom.201901471
73. Sheng Z, Hu D, Zheng M, et al. Smart human serum albumin-indocyanine green nanoparticles generated by programmed assembly for dual-modal imaging-guided cancer synergistic phototherapy. *ACS Nano*. 2014;8(12):12310–12322. doi:10.1021/nn5062386
74. Zhang Y, Jia Y, Zhu S. NIR-II cyanine@albumin fluorophore for deep tissue imaging and imaging-guided surgery. *SmartMat*. 2024;5(4):e1245. doi:10.1002/smm2.1245
75. Hu D, Zha M, Zheng H, Gao D, Sheng Z. Recent advances in indocyanine green-based probes for second near-infrared fluorescence imaging and therapy. *Research*. 2025;8:0583. doi:10.34133/research.0583
76. Ma R, Alifu N, Du Z, et al. Indocyanine green-based theranostic nanoplatform for NIR fluorescence image-guided chemo/photothermal therapy of cervical cancer. *Int J Nanomedicine*. 2021;17:4847–4861. doi:10.2147/IJN.S318678
77. Lin Q, Li C, Wang Y, Zhu Y, Gu Y. Discovery of near-infrared heptamethine cyanine probes for imaging-guided surgery in solid tumors. *J Med Chem*. 2024;67:5800–5812. doi:10.1021/acs.jmedchem.4c00010
78. Ding B, Xiao Y, Zhou H, et al. Polymethine thiopyrylium fluorophores with absorption beyond 1000 nm for biological imaging in the second near-infrared subwindow. *J Med Chem*. 2018;62:2049–2059. doi:10.1021/acs.jmedchem.8b01682
79. Guo L, Zhou Y, Ding J, et al. A near-infrared triggered multi-functional indocyanine green nanocomposite with NO gas release function inducing improved photothermal therapy. *J Colloid Interface Sci*. 2025;679:307–323. doi:10.1016/j.jcis.2024.10.071
80. Wang Y, Zhao G, Liu Y, et al. Glutathione-activated near-infrared II fluorescent probe for lung metastatic diagnosis and intraoperative imaging of tumor. *Sens Actuators B Chem*. 2025;426:137005. doi:10.1016/j.snb.2024.137005
81. Jia Q, Zhang R, Yan H, et al. An activatable near-infrared fluorescent probe for precise detection of the pulmonary metastatic tumors: a traditional molecule having a stunning turn. *Angew Chem*. 2023;135:e202313420. doi:10.1002/ange.202313420
82. Xu J, Du Y, Han T, Zhu N, Zhu S. Protein@cyanine-based NIR-II lymphography enables the supersensitive visualization of lymphedema and tumor lymphatic metastasis. *Adv Healthc Mater*. 2023;12:2301051. doi:10.1002/adhm.202301051
83. Barresi E, Baldanzi C, Roncetti M, et al. A cyanine-based NIR fluorescent vemurafenib analog to probe BRAFV600E in cancer cells. *Eur J Med Chem*. 2023;256:115446. doi:10.1016/j.ejmech.2023.115446
84. Zhang C, Liu T, Luo P, et al. Near-infrared oxidative phosphorylation inhibitor integrates acute myeloid leukemia–targeted imaging and therapy. *Sci Adv*. 2021;7:eabb6104. doi:10.1126/sciadv.abb6104
85. Gao G, Che J, Xu P, Chen B, Zhao Y. Biomimetic cell membrane decorated ZIF-8 nanocarriers with IR-780 and doxorubicin loading for multiple myeloma treatment. *Aggregate*. 2024;5:e631. doi:10.1002/agt2.631
86. Zou X, Zhao Y, Lin W. Photoacoustic/fluorescence dual-modality cyanine-based probe for real-time imaging of endogenous cysteine and in situ diagnosis of cervical cancer in vivo. *Anal Chim Acta*. 2023;1239:340713. doi:10.1016/j.aca.2022.340713
87. Tsuchiya K, Takakura H, Nakajima K, et al. Piperazine-based pH-responsive cyanine dyes for cancer cell photoacoustic imaging. *J Photochem Photobiol a Chem*. 2024;453:115634. doi:10.1016/j.jphotochem.2024.115634
88. Liu Y, Lu X, Zhou W, et al. Molecular engineering of a commercially available NIR-II fluorescent cyanine dye for improved tumor targeting and imaging. *New J Chem*. 2023;47:20088–20094. doi:10.1039/D3NJ03868H
89. Lyu S, Lu S, Gui C, et al. A NIR-II photoacoustic/NIR-IIa fluorescent probe for targeted imaging of glioma under NIR-II excitation. *J Med Chem*. 2024;67:1861–1871. doi:10.1021/acs.jmedchem.3c01515
90. Liu WL, Zhang YQ, Luo XJ, et al. Novel dual-mode NIR-II/MRI nanoprobe targeting PD-L1 accurately evaluates the efficacy of immunotherapy for triple-negative breast cancer. *Int J Nanomedicine*. 2023;18:5141–5157. doi:10.2147/IJN.S417944
91. Wang J, Yang L, Ding W, et al. Development of in vitro and in vivo c-Met targeted dual-modal nanoprobes for NIR-II fluorescent bioimaging and magnetic resonance imaging of breast carcinoma metastasis. *Arab J Chem*. 2024;17:105919. doi:10.1016/j.arabjc.2024.105919
92. Xu M, Lin Y, Li Y, et al. Nanoprobe based on novel NIR-II quinolinium cyanine for multimodal imaging. *Small*. 2024;20:2406879. doi:10.1002/smll.202406879
93. Zhu J, Liu Y, Li W, Xu C, Zhang T, Zhao H. In vivo evaluation of a gallium-68-labeled tumor-tracking cyanine dye for positron emission tomography/near-infrared fluorescence carcinoma imaging, image-guided surgery, and photothermal therapy. *ACS Omega*. 2023;8:6067–6077. doi:10.1021/acsomega.2c08235
94. Zhou J, Li H, Wu B, et al. Network pharmacology combined with experimental verification to explore the potential mechanism of naringenin in the treatment of cervical cancer. *Sci Rep*. 2024;14(1):1860. doi:10.1038/s41598-024-52413-9
95. Wang Y, Xu Y, Song J, et al. Tumor cell-targeting and tumor microenvironment–responsive nanoplatforms for the multimodal imaging-guided photodynamic/photothermal/chemodynamic treatment of cervical cancer. *Int J Nanomedicine*. 2024;19:5837–5858. doi:10.2147/IJN.S466042
96. Wang L, Zeng W, Long K, et al. Advances in photoacoustic imaging reconstruction and quantitative analysis for biomedical applications. *arXiv*. 2024;2411.02843. doi:10.48550/arXiv.2411.0284

97. Repetowski P, Warszyńska M, Dąbrowski JM. NIR-activated multifunctional agents for the combined application in cancer imaging and therapy. *Adv Colloid Interface Sci*. 2024;336:103356. doi:10.1016/j.cis.2024.103356
98. Yuan J, Yang H, Huang W, et al. Design strategies and applications of cyanine dyes in phototherapy. *Chem Soc Rev*. 2025. doi:10.1039/D3CS00585B
99. Liu J, Wang F, Qin Y, Feng X. Advances in the genetically engineered KillerRed for photodynamic therapy applications. *Int J Mol Sci*. 2021;22(18):10130. doi:10.3390/ijms221810130
100. Alves CG, Lima-Sousa R, de Melo-Diogo D, Louro RO, Correia IJ, Santos AC. IR780-based nanomaterials for cancer imaging and photothermal, photodynamic and combinatorial therapies. *Int J Pharm*. 2018;542:164–175. doi:10.1016/j.ijpharm.2018.03.020
101. Zhao X, Du J, Sun W, et al. Regulating charge transfer in cyanine dyes: a universal methodology for enhancing cancer phototherapeutic efficacy. *Acc Chem Res*. 2024;57:2582–2593. doi:10.1021/acs.accounts.4c00399
102. Cheng L, He WW, Gong H, et al. PEGylated micelle nanoparticles encapsulating a non-fluorescent near-infrared organic dye as a safe and highly-effective photothermal agent for in vivo cancer therapy. *Adv Funct Mater*. 2013;23:5893–5902. doi:10.1002/adfm.201301045
103. Zhao X, He S, Chi W, et al. An approach to developing cyanines with upconverted photosensitive efficiency enhancement for highly efficient NIR tumor phototheranostics. *Adv Sci*. 2022;9:2202885. doi:10.1002/advs.202202885
104. Yue CX, Liu P, Zheng MB, et al. IR-780 dye-loaded tumor targeting theranostic nanoparticles for NIR imaging and photothermal therapy. *Biomaterials*. 2013;34:6853–6861. doi:10.1016/j.biomaterials.2013.05.071
105. Kejík Z, Hajduch J, Abramenko N, et al. Cyanine dyes in the mitochondria-targeting photodynamic and photothermal therapy. *Commun Chem*. 2024;7:180. doi:10.1038/s42004-024-01256-6
106. Ma J, Jiang L. Photogeneration of singlet oxygen ($^1O_2$) and free radicals ($Sen^-$, $O_2^-$) by tetra-brominated hypocrellin B derivative. *Free Radic Res*. 2001;35:767–777. doi:10.1080/10715760100301271
107. Zhang Y, Zhao M, Miao J, et al. Hemicyanine-based type I photosensitizers for antihypoxic activatable photodynamic therapy. *ACS Mater Lett*. 2023;5:3058–3067. doi:10.1021/acsmaterialslett.3c00933
108. Bel'ko N, Mal'tanova A, Bahdanava A, et al. Near-infrared superoxide generator based on a biocompatible indene-bearing heptamethine cyanine dye. *J Mater Chem B*. 2024;4:11202–11209. doi:10.1039/D4TB01663G
109. Song F, Peng X, Lu E, et al. Syntheses, spectral properties and photostabilities of novel water-soluble near-infrared cyanine dyes. *J Photochem Photobiol a Chem*. 2004;168:53–57. doi:10.1016/j.jphotochem.2004.05.012
110. Yi M, Xiong B, Li Y, et al. Manipulate tumor hypoxia for improved photodynamic therapy using nanomaterials. *Eur J Med Chem*. 2023;247:115084. doi:10.1016/j.ejmech.2022.115084
111. Lu B, Wang L, Tang H, et al. Recent advances in type I organic photosensitizers for efficient photodynamic therapy for overcoming tumor hypoxia. *J Mater Chem B*. 2023;11:4600–4618. doi:10.1039/D3TB00545C
112. Lange N, Szlasa W, Saczko J, et al. Potential of cyanine derived dyes in photodynamic therapy. *Pharmaceutics*. 2021;13:818. doi:10.3390/pharmaceutics13060818
113. Liu J, Wang L, Shen R, et al. A novel heptamethine cyanine photosensitizer for FRET-amplified photodynamic therapy and two-photon imaging in A-549 cells. *Spectrochim Acta A Mol Biomol Spectrosc*. 2022;274:121083. doi:10.1016/j.saa.2022.121083
114. Santos PF, Reis LV, Almeida P, Fernandes R, Tomé JPC, Cavaleiro JAS. Singlet oxygen generation ability of squarylium cyanine dyes. *J Photochem Photobiol a Chem*. 2003;160:159–161. doi:10.1016/S1010-6030(03)00203-X
115. Liang M, Mu X, Li Y, et al. Heptamethine cyanine-based nanotheranostics with catalase-like activity for synergistic phototherapy of cancer. *Adv Funct Mater*. 2023;33:2302112. doi:10.1002/adfm.202302112
116. Bhattarai P, Dai Z. Cyanine based nanoprobes for cancer theranostics. *Adv Healthc Mater*. 2017;6:1700262. doi:10.1002/adhm.201700262
117. Deng X, Shao Z, Zhao Y. Solutions to the drawbacks of photothermal and photodynamic cancer therapy. *Adv Sci*. 2021;8(3):2002504. doi:10.1002/advs.202002504
118. Yang W, Wang N, Yang J, et al. A multifunctional 'golden cicada' nanoplatform breaks the thermoresistance barrier to launch cascade augmented synergistic effects of photothermal/gene therapy. *J Nanobiotechnology*. 2023;21:228. doi:10.1186/s12951-023-01983-3
119. Wang C, Xu L, Liang C, Xiang J, Peng R, Liu Z. Immunological responses triggered by photothermal therapy with carbon nanotubes in combination with anti-CTLA-4 therapy to inhibit cancer metastasis. *Adv Mater*. 2014;26:8154–8162. doi:10.1002/adma.201402996
120. Zhang F, Cao J, Chen X, Zhang X, Zhu Z, Shen B. Noninvasive dynamic imaging of tumor early response to nanoparticle-mediated photothermal therapy. *Theranostics*. 2015;5:1444. doi:10.7150/thno.13398
121. Wang W, Zhang Y, Zhang Y, et al. Biomimetic liposomes as a pH/ROS cascade-responsive nanoagent with high selectivity for breast carcinoma in photothermal therapy. *Mater Des*. 2023;234:112304. doi:10.1016/j.matdes.2023.112304
122. Feng E, Lv F, Tang S, et al. The unexpected "butterfly effect" of Pt-coordinated cyanine self-assembly for enhanced tumor photothermal therapy. *Sci China Mater*. 2024;67:3003–3011. doi:10.1007/s40843-024-2976-8
123. Yang H, Yuan W, Cao J, et al. Poly(dopamine) coated H-aggregates of amphoteric charged near-infrared absorbing cyanine dyes for enhanced photothermal tumor imaging and therapy. *Dyes Pigm*. 2024;226:112141. doi:10.1016/j.dyepig.2024.112141
124. Kim JY, Choi WI, Kim M, Tae G, Kim YH, Choi Y. Tumor-targeting nanogel that can function independently for both photodynamic and photothermal therapy and its synergy from the procedure of PDT followed by PTT. *J Control Release*. 2013;171:113–121. doi:10.1016/j.jconrel.2013.07.006
125. Liu T, Chen Y, Wang H, et al. Phototheranostic agents based on nonionic heptamethine cyanine for realizing synergistic cancer phototherapy. *Adv Healthc Mater*. 2023;12:2202817. doi:10.1002/adhm.202202817
126. Li Y, Zhang J, Zhu L, et al. All-in-one heptamethine cyanine amphiphiles for dual imaging-guided chemo-photodynamic-photothermal therapy of breast cancer. *Adv Healthc Mater*. 2023;12:2300941. doi:10.1002/adhm.202300941
127. Gu QS, Li T, Wang WX, et al. A tumor-targeting fluorescent probe for ratiometric imaging of pH and improving PDT/PTT synergistic therapy. *Sens Actuators B Chem*. 2023;393:134287. doi:10.1016/j.snb.2023.134287
128. Yu Y, Wang H, Zhuang Z, et al. Self-adaptive photodynamic-to-photothermal switch for smart antitumor photoimmunotherapy. *ACS Nano*. 2024;18:13019–34. doi:10.1021/acsnano.4c01600
129. Juaim AN, Sun J, Nie R, et al. IR820 sensitized ceria nanozyme via PDA bridging for multifaceted antibacterial wound healing therapy. *Small*. 2025;21:2500382. doi:10.1002/smll.202500382

130. Pflug KM, Lee DW, Tripathi A, et al. Cyanine dye conjugation enhances crizotinib localization to intracranial tumors, attenuating NF-κB-inducing kinase activity and glioma progression. *Mol Pharm*. 2023;20:6140–6150. doi:10.1021/acs.molpharmaceut.3c00496
131. Al-Ghabkari A, Huang B, Park M. Aberrant MET receptor tyrosine kinase signaling in glioblastoma: targeted therapy and future directions. *Cells*. 2024;13:218. doi:10.3390/cells13030218
132. Chen M, Fu Y, Liu Y, et al. NIR-light-triggered mild-temperature hyperthermia to overcome the cascade cisplatin resistance for improved resistant tumor therapy. *Adv Healthc Mater*. 2024;13:2303667. doi:10.1002/adhm.202303667
133. Hamaya S, Oura K, Morishita A, et al. Cisplatin in liver cancer therapy. *Int J Mol Sci*. 2023;24:10858. doi:10.3390/ijms241310858
134. Wang SZ, Guo Y, Zhang X, et al. Mitochondria-targeted photodynamic and mild-temperature photothermal therapy for realizing enhanced immunogenic cancer cell death via mitochondrial stress. *Adv Funct Mater*. 2023;33:2303328. doi:10.1002/adfm.202303328
135. Yu JF, Wen Y, Li M. An active self-mitochondria-targeting cyanine immunomodulator for near-infrared II fluorescence imaging-guided synergistic photodynamic immunotherapy. *Adv Healthc Mater*. 2024;13:2401061. doi:10.1002/adhm.202401061
136. Song G, Zeng C, Li J, et al. Exosome-based nanomedicines for digestive system tumors therapy. *Nanomedicine*. 2025;20(10):1167–1180. doi:10.1080/17435889.2025.2493037